PERMANENT MOLD FORMATION USING ADDITIVE MANUFACTURING TECHNIQUES

A Dissertation Proposal
Submitted
By

Jatin Manchanda
(11000745)

to

Department of Mechanical Engineering

In partial fulfilment of the Requirement for the
Award of the Degree of

Masters of Technology in Mechanical Engineering

Under The Guidance of
Mr. Gurpreet Singh Phull

(APRIL, 2015)

DECLARATION

I hereby declare that the dissertation proposal entitled, **PERMANENT MOLD FORMATION USING ADDITIVE MANUFACTURING TECHNIQUES** submitted for the M.Tech Degree is entirely my original work and all ideas and references have been duly acknowledged. It does not contain any work for the award of any other degree or diploma.

Date:-__ __ ____

JATIN MANCHANDA

(Reg no. 11000745)

CERTIFICATE OF THE GUIDE

This is to certify that the declaration statement made by the student is correct to the best of my knowledge and belief. I assure all the contents, research work, analysis, and interpretations are genuine attempt on his part. The Dissertation Project Proposal based on the technology / tool learnt is fit for the submission and partial fulfilment of the conditions for the award of M.Tech in mechanical engineering from Lovely Professional University, Phagwara.

Name: ……..

U.ID: ……

Designation: ……

Signature of Faculty Mentor

ABSTRACT

Permanent mold is a reusable hollowed block used to shape a deformable material into the particular shape which it possess within its cavity. Rapid prototyping is a group of practices used to rapidly fabricate a physical model of a part or assembly using three dimensional computer aided design (CAD) data. Electroplating is a process that uses electric current to dissolve one electrode into its salt and hence cohere the dissolved metal ions on another electrode of equal or higher nobility. Cold spray is from the family of thermal spray technology with the distinction that it is a solid state process in which the spray particles are deposited by means of supersonic velocity impact at a temperature much lower than the melting point of the spray material. This study invokes the process and related considerations for formation of permanent mold dies incorporating rapid prototyping, electroplating and cold thermal spraying techniques. The method to be undertaken in the said research involves the development of such a technique for fabrication of molds which is cheap, easy and virtually independent of the complexity of the pattern shape.

ACKNOWLEDGEMENT

Gratitude is the hardest of emotions to express, often one doesn't find adequate words to convey the feeling of gratefulness. There were many people whom I would like to thank for their support. I sincerely feel that credit of this work could not be narrowed down to any one individual, by which I have achieved its completion.

I take this opportunity to express my intense gratitude and profound regards to my mentor Mr. Gurpreet Singh Phull for his exemplary guidance, monitoring and constant encouragement throughout the course of this research project. Whole tenure of the project was a keen learning experience not only in terms of academics but also in social behavioral; because of him. The blessing, help and guidance given by him time to time is definitely going to take me long way in the journey of life on which I am about to embark.

I am obliged to my co-mentor Mr. Harpinder Singh Sandhu for his direct involvement, immense guidance and relentless encouragement which not only invoked new ideas in me, but also puffed me with zeal to give new dimensions to the study. His sincere advices were never confined to this particular project but are extended for various other endeavors which are waiting my way in the industry. His comments has always been proven noteworthy.

I am thankful to all the staff members of the university, for the appreciable information provided by them in their respective fields. I am grateful for their cooperation during the period of this study.

I would also like to acknowledge the dedication and enthusiasm of my team members Aditya, Ashish, Ashutosh, Atul and Devesh, which not only led to the completion of the study but also fortified me in various stages.

I further extend my heartiest gratitude to the members of the student organization LPU-SAE India Collegiate Club (LSCC) for their selfless help in my project.

Next, the acknowledgement worth people are my friends who constantly helped and suggested me various ideas to make up with the project. Their advices were enormously valuable.

I further thank all the people who were directly or indirectly connected to the project without them the work wouldn't have been in the conclusive state.

CONTENTS

LIST OF FIGURES

LIST OF TABLES

CHAPTER-I (INTRODUCTION)

The topic of study is 'FORMATION OF PERMANENT MOLDS USING ADDITIVE MANUFACTURING TECHNIQUES.' The study is based on finding the appropriate techniques and procedures of additive manufacturing to form permanent molds.

Presently the permanent molds for plastic and metal casting are made by metal removal processes such as milling etc., which consume a lot of time and capital resources. If the design of the product is a bit more complex it further adds up to the time as well as the cost incurred in making the molds. This directly affects the price of consumer product. The advanced technology is not only the one which produces something in a new way but which makes something in new as well as efficient way. This research has the potential to make a breakthrough in the mold making technologies. The method to be undertaken in the said research involves the development of such a technique which is cheap, easy and virtually independent of the complexity of the part shape.

The study is based upon adding material rather removing; to make the molds which adversely reduces the time and material wastage and hence saves the capital resources required for the fabrication. In this study, Fused Deposition Modelling (FDM); a rapid prototyping technique is being used to make patterns and cold spray technique; a thermal spray technology is being used to deposit thick layers of metal over pattern to make the dies.

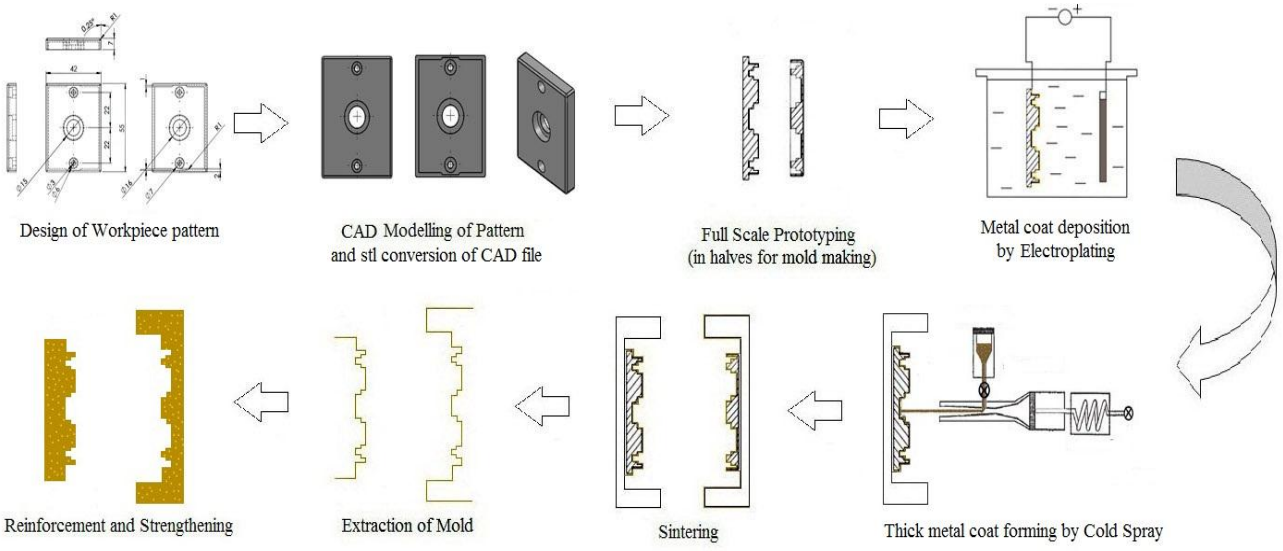

FIGURE 1 SCHEMATIC FLOW CHART SHOWING CONCEPT OF STUDY

1.1 INTRODUCTION TO MOLDS

Permanent mold is a reusable hollowed block used to shape a deformable material into the particular shape which it possess within its cavity.

Permanent molds are employed for casting of both metals and non-metals. As the name suggests, permanent molds are reusable molds usually made from metals. Application of permanent molds is not limited to the casting of materials like aluminum, magnesium, copper alloys, tin, zinc, lead alloys, and iron, and steels but these are also used for injection molding and blow molding of plastics and rubber. Typical parts that are made by molding are gears, wheels, housings, pipe fittings, casings, tires, pet bottles etc.

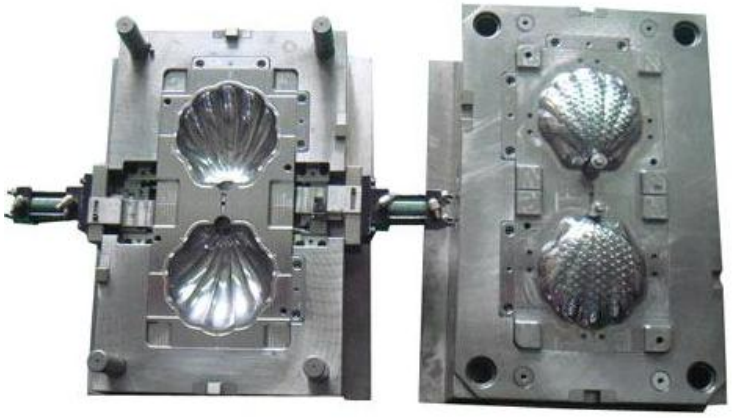

FIGURE 2 PERMANENT MOLDS (USED FOR PLASTIC INJECTION MOLDING) [1]

Molding is a manufacturing technique to shape a deformable material into desired attributes which are carved over the mating faces of the molds. Types of molding includes;

- Blow molding
- Powder metallurgy plus sintering
- Compression molding
- Extrusion molding
- Injection molding
- Matrix molding
- Plastic molding
- Rotational molding (or Rotomolding)
- Spin casting
- Transfer molding
- Thermoforming

1.2 INTRODUCTION TO ADDITIVE MANUFACTURING

1.2.1 RAPID PROTOTYPING

Rapid prototyping [2] (most recently, broadly classified as additive manufacturing) is a group of techniques used to rapidly fabricate a physical model of a part or assembly employing three-dimensional computer aided design (CAD) data. Rapid prototyping (RP) technologies can automatically construct physical prototypes from Computer-Aided Design (CAD) data. The main advantage of the system is that almost any shape can be produced. These techniques are solid free-form fabrication techniques that layer manufacture the prototypes by making the use of computer automated manufacturing. The computer aided design model is divided into thin layers and the part is made-up by adding layers over one-another.

The procedural work of Rapid Prototyping can be understood as under:-

- Firstly, the CAD model is prepared using available CAD software packages such as Pro-Engineer, Creo-Parametric, Solid Works, CATIA, etc.
- Then, the CAD model is converted to 'Sliced Thin Layer (SLT)' format.
- The SLT format file is fed into the software interface of the prototyping machine.
- Afterwards the required scaling and orientation is set and the final commands are given.
- Machine software analyze the model and converts the data into machine hardware language; determining the tool motion path.
- The tool then moves as according to the tool motion path; adding the material layer upon layer to produce actual physical model from the CAD data.

Most rapid prototyping techniques use plastics as their material; but direct use of metals in form of powders and strips is also not an evaded field.

RAPID PROTOTYPING TECHNIQUES

The rapid prototyping techniques [3, 4] finds their classifications as mentioned under:-

- Stereo lithography (SLA)
- Selective Laser Sintering (SLS)
- Laminated Object Manufacturing (LOM)
- 3D Printing (3DP)
- Direct metal laser sintering (DMLS)
- Fused Deposition Modeling (FDM)

STEREOLITHOGRAPHY

Stereo lithography is vastly used prototyping technology. It can produce very accurate and detailed polymer parts. Stereo lithography was the first rapid prototyping process. It was introduced by 3D Systems Inc. in 1988.

Stereo lithography uses a low-power Ultra violet laser which is extremely focused, to yield a three dimensional entity in a vessel of photosensitive liquid polymer.

TABLE 1 PROPERTIES OF STEREOLITHOGRAPHY

Material type:	Liquid (Photopolymer)
Materials:	Thermoplastics (Elastomers)
Minimum layer thickness:	0.02mm
Surface finish:	Smooth
Build speed:	Average

SELECTIVE LASER SINTERING

The elementary theory behind selective laser sintering technology is akin to that of Stereo lithography. It uses a laser beam that moves to trace the tool path to selectively sinter the powdered metal, composite materials and/or polymer. It was patented in 1989.

TABLE 2 PROPERTIES OF SELECTIVE LASER SINTERING

Material type:	Powder(Polymer)
Materials:	Nylon, Polyamide, Polystyrene and Composites
Minimum layer thickness:	0.10mm
Surface finish:	Average
Build speed:	Fast

LAMINATED OBJECT MANUFACTURING

The laminated object manufacturing system contains feeding mechanism that lays a sheet over the build platform, a heater roller to apply pressure in order to glue the top layer to the bottom layers. A laser is used to cut the periphery of the part in each layer of sheets. On completion of each cut, the platform is dropped by a distance equivalent to the thickness of the sheet. The laser cuts the periphery

of each layer until the part is completed. After cutting a layer, the extra material is not removed in order to support the part.

TABLE 3 PROPERTIES OF LAMINATED OBJECT MANUFACTURING

Material type:	Solid sheets
Materials:	PVC, Paper, Composites, Ferrous metals, Non-ferrous metals, Ceramics
Minimum layer thickness:	0.05mm
Surface finish:	Rough
Builds peed:	Fast

THREE DIMENSIONAL PRINTING

Three dimensional printing process is similar to the selective laser sintering, with a distinction that rather using a laser to sinter the material, an ink-jet printing head is used to deposit a liquid adhesive that glues the material. Three dimensional printing technology was developed at the MIT.

Three dimensional printing is advantageous in terms that it is comparatively inexpensive than other additive processes but the material options are limited. Three dimensional printing is a fast technology that can print 2 –4 layers/minute. Compared to other rapid prototyping processes, it lags behind in the part strength, accuracy, and the surface finish. More over the final part is required to be reinforced with a sealant to mend strength and surface finish.

TABLE 4 PROPERTIES OF THREE DIMENSIONAL PRINTING

Material type:	Powder
Materials:	Stainless steel, Bronze, Composites, Elastomers, and Ceramics
Minimum layer thickness:	0.05mm
Surface finish:	Rough
Build speed:	Very Fast

DIRECT METAL LASER SINTERING

Direct metal laser sintering was the first commercially used prototyping method that is capable of producing metal parts in a single process. It was developed by Rapid Prototyping Innovations (RPI) and EOS Gmbhin, cooperatively in 1994. In this technology, the metal powder are directly melted

by skimming of a high power laser beam, without incorporating any sort of binders. Direct metal laser sintering is advantageous over other additive processes as it produces high density part of portion up to 98 %. Moreover, since the size of raw material particles is very small, enormously detailed parts can be made using this technology.

TABLE 5 PROPERTIES OF DIRECT METAL LASER SINTERING

Material type:	Metal Powder
Materials:	Aluminum, Bronze, Cobalt-chrome Steel alloys, Stainless steel, Tool steel, Titanium, Ceramics.
Minimum layer thickness:	0.02mm
Surface finish:	Average
Build speed:	Fast

FUSED DEPOSITION MODELING

In fused deposition modeling process, a wax or plastic material is extruded from a nozzle that follows the peripheral geometry of the part layer-wise. It was developed by Stratasys.

TABLE 6 PROPERTIES OF FUSED DEPOSITION MODELING

Material type:	Solid Filaments
Materials:	ABS, Polyphenylsulfonite, Polycarbonate, Elastomers
Minimum layer thickness:	0.15mm
Surface finish:	Rough
Build speed:	Slow

The FDM machine [5] have a mobile head which deposits the extruding filaments of the molten plastic on a surface. The building material at the extruder nozzle is heated beyond 0.5°C to its melting point for the cause that it sets solid after extrusion within 0.1 s and adheres to the former layers. The overall layer thickness is adversely affected by the factors such as material extrusion rate, nozzle speed, and the speed of the head [6, 7].

PROCESS OF FUSED DEPOSITION MODELING [8, 9]

Fused deposition modeling initiates with a software practice in which the CAD model of prototype is converted into Sliced Thin Layer (STL) format as in case of the most of rapid prototyping techniques. STL conversion is the process of mathematical slicing and positioning of the model for the build process. On the software end, the support structures are also generated as per the requirements, while conversion into STL format.

The part is formed by extruding tiny blobs of thermoplastic material to produce layers as the material solidifies instantly after extrusion from the nozzle. The machine is capable of dispensing multiple materials; one to shape up the model and another as a fragile structure for support. Plastic strands are forced into the hot extruder nozzle where they melt due to heating beyond their glass transition temperature. Normally, a worm-drive is employed to force the filament into the nozzle at a regulated speed. Then the molten blobs are deposited by extrusion head. The stimulation of nozzle can be done in both vertical and horizontal directions by a numeric control mechanism. It tracks a tool-path generated by a computer-aided manufacturing (CAM) software package. The part is erected from the bottom to top, layer by layer.

Fused deposition modelling is very lithe technology. It is capable of generating parts with minor overhangs by the backing from bottom layers.

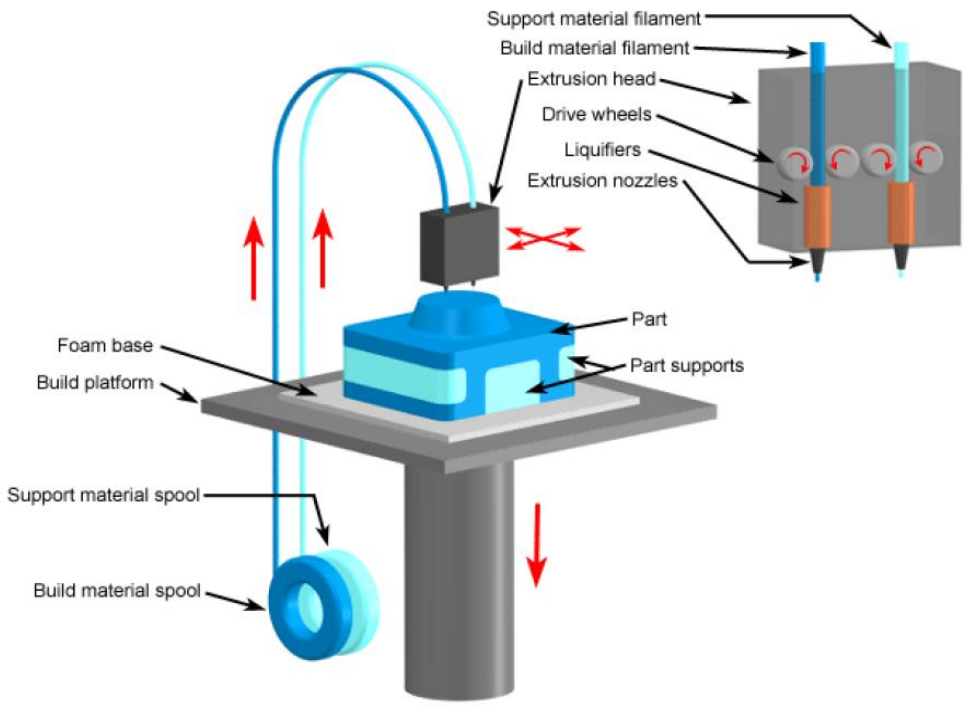

FIGURE 3 EQUIPMENT FOR FUSED DEPOSITION MODELLING [10]

1.2.2 ELECTROPLATING

Electroplating is a process that uses electric current to dissolve one electrode into its salt and hence cohere the dissolved metal ions on another electrode of equal or higher nobility. This process is akin to the process of galvanic cell but working reversely. In this process, the two electrodes are immersed in an electrolytic solution that is usually the salt of the material that is required to be deposited (Copper Sulphate in case of copper plating). The part which is required to be plated is the cathode (+) and the material of plating is the anode (-) in the circuit. It is required that the part which is to be coated should either be equal or greater in terms of nobility in the galvanic series. A direct current power supply is attached to the circuit which forces oxidation at the anode and reduction at the cathode. The electric current dissolves the metal from anode into the electrolytic solution and deposits it on the cathode workpiece. The rate of oxidation and reduction reactions are always equal which ensures the replenishment of ions in the solution bath. [71]

PROCESS OF COPPER ELECTROPLATING

In the electrolytic $CuSO_4$ solution, Cu is oxidized from the copper anode to Cu^{2+} by giving two electrons to the power supply. The Cu^{2+} ions hence loosens and dissolves in the solution, then they links with the anion SO_4^{2-} already present in the solution to form $CuSO_4$. At the cathode, the Cu^{2+} is reduced to metallic Cu by the gain of two electrons from the power supply. In this way, the total number of electrons and Cu^{2+} and SO_4^{2-} ions are replenished in the system further resulting in coating of Cu metal plate over the cathode. [72]

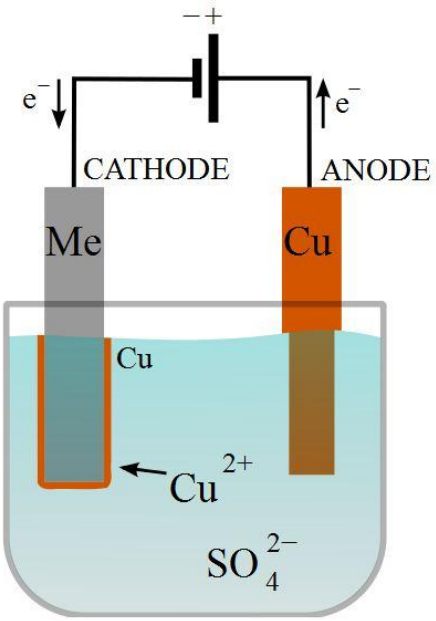

FIGURE 4 SCHEMATIC OF ELECTROPLATING PROCESS

1.2.3 THERMAL SPRAYING

Thermal spraying technologies [13, 14, 15] are constituents of the group of coating technologies that are used to deposit thick layers of ceramic, metallic, cermet, alloys, plastics, or even composite materials. Thermal spraying can provide thick coatings ranging from 50 μm to 1 mm, over a large area at a high rate of deposition; compared to other coating processes such as cladding, electroplating, glazing, and vapor deposition. The materials are served in powder or wire form, heated to a molten, semi molten state, or even in solid-state and accelerated towards the substrates in form of tiny particles. The particles bombard the substrate, and due to impact, gets flatten, and form tinny splats that imitate and adhere to the substrate surface and to each other. As the sprayed particles strikes upon the surface, they build up to form a laminar structure, splat by splat, termed as thermal spray coating.

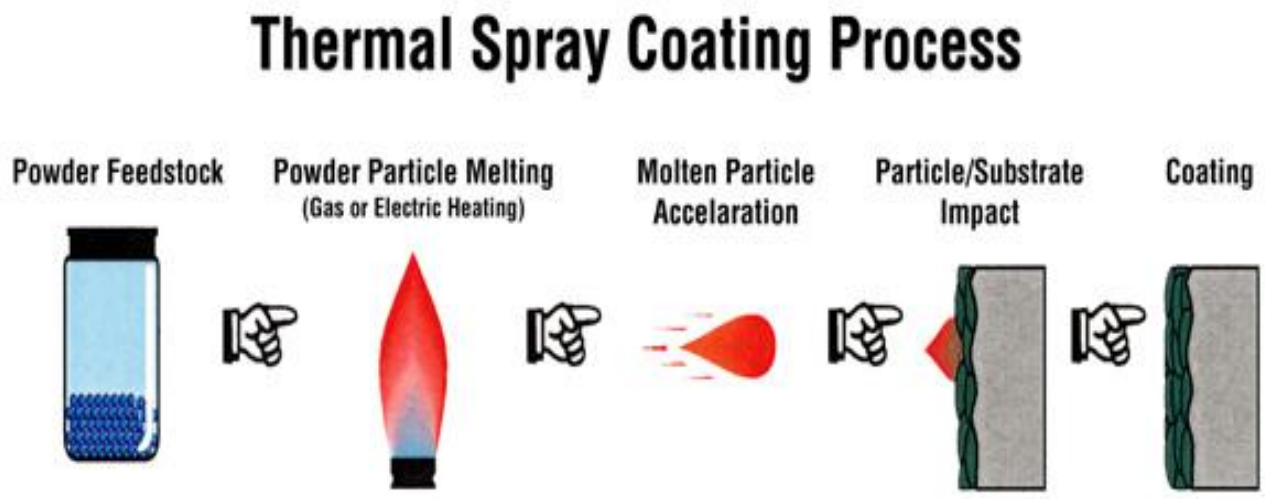

FIGURE 5 SCHEMATIC OF THERMAL SPRAYING PROCESS

TYPES OF THERMAL SPRAYING [16]

- Flame thermal spraying
- Plasma thermal spraying
- Wire arc thermal spraying
- Detonation thermal spraying
- High velocity oxy-fuel thermal spraying
- Warm thermal spraying
- Cold spraying

Flame spraying

In wire or rod flame spraying, the spray material is constantly melted in the middle of an oxy-acetylene flame. The molten metal hence formed is sprayed in the form of droplets with the help of an atomizing gas such as compressed air or nitrogen. The molten particles are discharged from the melting zone and impelled onto the workpiece surface. Flame spraying with wire as its material is widely used in the automotive industry to smear a very high superiority coating of molybdenum over gear selectors, piston rings and the synchronizing rings.

Plasma Spraying

In plasma spraying process, a plasma jet is emanated from a plasma torch, in which the material to be deposited is either served as a powder or wire form. The temperature in the jet usually reaches to the order of 10,000K which melts and propels the material towards the substrate. At the substrate surface, the molten metal droplets gets flatten and solidifies rapidly to form a deposit, which remain adherent to the substrate as coat. Plasma spraying finds its application in producing free-standing parts by removing the substrate after spray.

Wire arc spraying

In wire arc spraying, two similar or different types of feedstock metal wires are continuously fed to bring them closer so as to passing high currents from them to form an arc. At the tip of the arc, the wires are melted off and are propelled onto the workpiece surface by employment of an atomizing gas, e.g. compressed air. Wire arc spraying is a high-performance wire spraying process. In wire arc spraying, only electrically conductive materials can be used for feedstock. Wire arc spraying finds their applications in anti-corrosion protection, large-area coating of vessels, bond coatings, cylinder liners, etc.

Detonation Spraying

The Detonation spraying apparatus has a gun with long water-cooled barrel having inlet valves for the gases and the material powder. In this process, a charge of powder is fed into the barrel along with oxygen and fuel. A spark ignites the mixture to create detonation in the chamber. The resulting detonation heats and accelerates the powder to supersonic velocities through the barrel. After each detonation, a pulse of nitrogen is used to purge the barrel. The process is usually repeated many times in a second. High kinetic energy of hot particles do result in the buildup of a very strong and dense coating, on impact with the substrate.

High velocity oxygen fuel spraying (HVOF)

In High velocity oxygen fuel spraying technology, a mixture of oxygen and fuel is served into a combustion chamber, where ignition occurs. This causes development of high pressure (up to 1MPa) which emanates through a nozzle. The jet velocity at the exit of the barrel becomes supersonic. Metal powder is fed into the gas stream, which accelerates up to 800m/s. The hot gas and particle containing stream is focused towards the surface of the substrate. The powder melts partially in the stream, and deposits low porosity and high bond strength coating upon the substrate. The fuels that can be used in HVOF can be gases or liquids.

Warm spraying

It is an alteration in HVOF spraying. In warm spraying, nitrogen gas is mixed with the combustion gas to lower down its temperature. The mixture gas usually contains much unreacted hydrocarbons water vapor, and oxygen but still, the coating efficiency is higher as compared to that of HVOF. The chemical reactions and melting of the feed powder are largely reduced due to lower temperatures in the process. Warm spraying is advantageous for coating such materials as Titanium, metallic glasses, and plastics which are vulnerable to oxidization and deterioration at elevated temperatures.

COLD SPRAY

Cold spray [17] is the type of thermal spray technology, in which metallic or sometimes even non-metallic particles are deposited over the substrate in solid state form. In this technology, the solid-state particles are accumulated in a coat using supersonic velocity impact rather deposition by solidification of molten or semi-molten particles as in other thermal spray processes.

Cold spray or more precisely, Gas dynamic cold spray (GDCS) is a solid state coating deposition method. The solid powders of diameter up to 60 micrometers in supersonic gas jets, are accelerated to velocities up to 400–1000 m/s. The particles undergo plastic deformation, during impact with the substrate, and due to transition of kinetic energy into strain energy, bonds to the surface. Metals, composite materials, and polymers can be deposited using this technology. The supplied kinetic energy by the expansion of the gas, of the particles, is transformed to plastic deformation energy during bonding.

Systems of cold spraying

The cold spray technology comprises of two types of systems that are nomenclature as the high-pressure cold spray system and the low-pressure cold spray system (shown in figure 8). The

operating principle for both the systems is very similar irrespective of the distinction of construction and the gas pressure.

TABLE 7 LOW PRESSURE AND HIGH PRESSURE COLD SPRAYING TECHNIQUES

Characteristics	Low Pressure Cold Spray	High Pressure Cold Spray
Gas Temperature (^{0}C)	Up to 550	550-1000
Gas Velocity (m/s)	300 to 600	1000 to 1400
Gas Pressure (bar)	5 to 25	25 to 30
Particle size (µm)	1 to 50	5 to 50
Particle Velocity (m/s)	300–600	500-1200
Splat Size (µm)	1 to 50	5 to 50
Nozzle distance (mm)	5-25	5-25
Coating Thickness (mm)	0.5-30	0.5-50
Spray Rate (kg/h)	3-15	10-30
Bond Strength (Mpa)	10-42	10-64
Spray Efficiency (%)	50	90

Equipment of cold spraying

The Cold Spray equipment can be either portable (manual) or fixed (robotic). Whichever the system may be, gas heater is mandatorily clubbed in order to heat the gas prior in order to reimburse for the cooling due to rapid expansion in the nozzle.

The main components (shown in figures 8 and 9) of Cold Spray apparatus (for both low pressure and high pressure cold spray systems) includes:

- Supersonic nozzle (De-Laval nozzle)
- Gas compressor
- Gas heater
- Powder feeder mechanism
- Mechanism for monitoring and controlling of the spray parameters

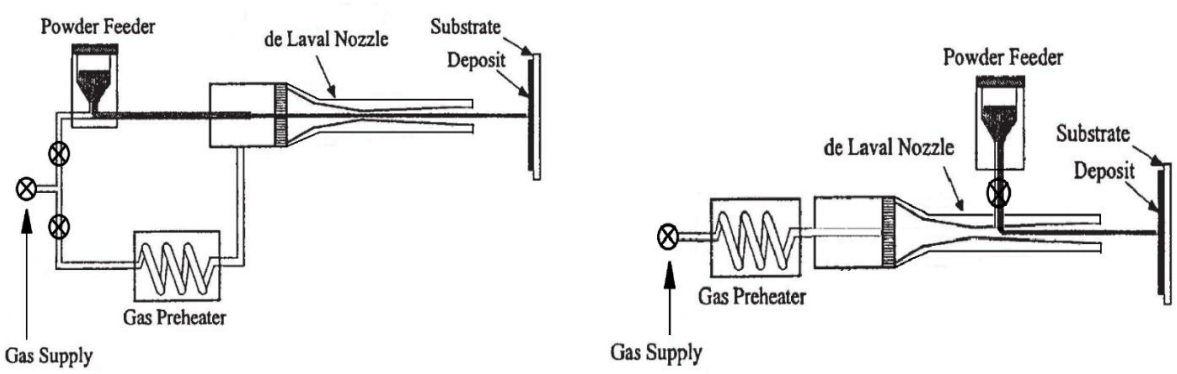

FIGURE 6 COLD SPRAY APPARATUS (HIGH VELOCITY & LOW VELOCITY RESPECTIVELY)

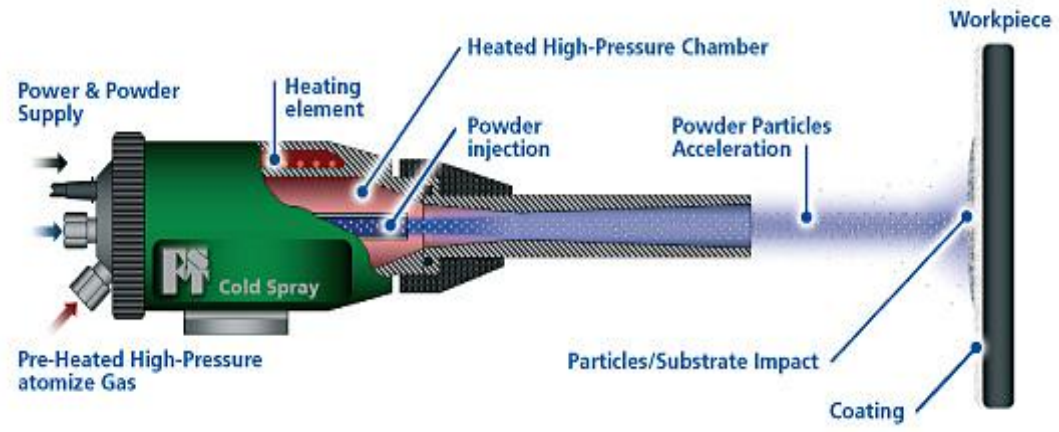

FIGURE 7 COLD SPRAY GUN

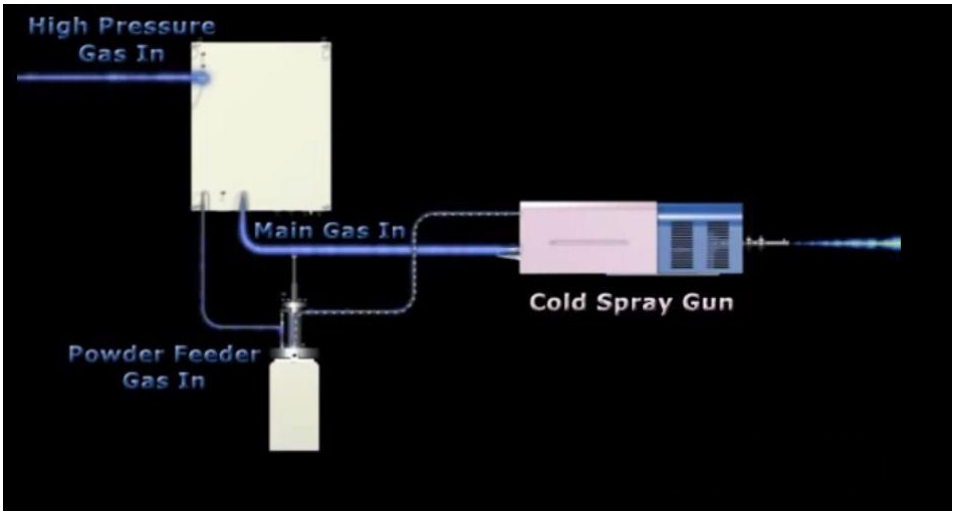

FIGURE 8 THE COLD SPRAY SYSTEM

Mechanism of Cold Spray

The principle behind cold spray process could easily be understood by the following explanation: A high velocity gas jet of order 350 to 1200 m/s is formed using a converging-diverging nozzle (usually a de Laval nozzle). The jet of gas thus formed is used to accelerate the tiny powder particles of diameter 1 to 60 μm in order to spray them onto a substrate. The substrate is required to be located 15-30 mm from nozzle's exit. The powder particles bombard over the substrate, and deform plastically into splats to adhere to the surface and to each other due to particles' kinetic energy rather than the high temperatures thereby minimizing the inadequacies associated with conventional thermal spray approaches such as oxidation, melting, evaporation, recrystallization, and residual stresses. The gasses with aerodynamic properties such as Helium, Nitrogen, mixture of Helium and Nitrogen or sometimes dry air; are largely used to propel the powder particles over the substrate. The bonding mechanism in the process can be easily understood by means of the most putative theory that during the impact, plastic deformation of solid particles occurs. Bombarding particles upsets reedy surface layers, which usually are of metal oxide, to attain close conformal contact. The high contact pressure involved indorses coalescence with the substrate surface. Champagne at al. in his experimentation observed the common phenomena during spraying onto numerous substrates, that the deformation of the substrate and the particle occurs showing viscous fluid-like behavior. On collision of spray material particles, metal jet formation is evident as a consequence of occurrence of interfacial waves, roll-ups, and vortices over the substrate [18]. The following figure could more easily comprehend this:-

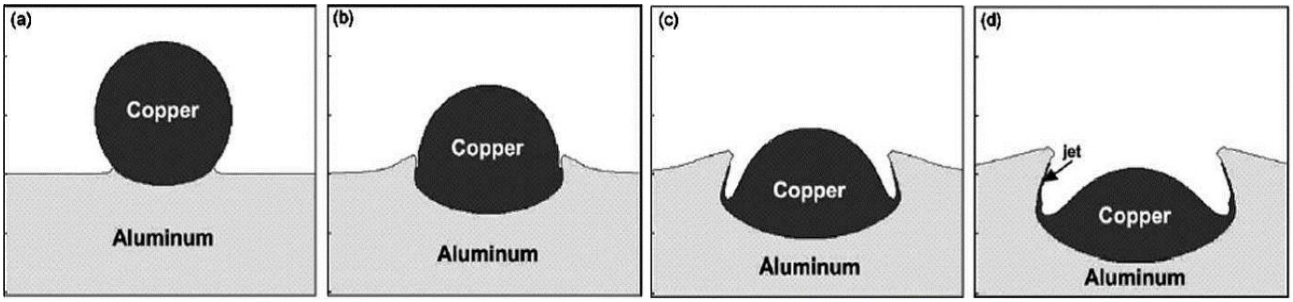

FIGURE 9 IMPACT OF PARTICLE ON SUBSTRATE AT SUCCESSIVE TIMES

H. Singh and M. E.Dickinson suggests through their research work that the particles' adhesion-strength of the in the process is exclusively dependent upon the kinetic energies at the impact time. The kinetic energies of the particles is characteristically much lower than the energy of melting and therefore cold spray is considered to be a process in solid-state [19, 20]. The notion is clarified by the Energy dispersive spectrometry image (Figure 9) of copper coating by cold spray on aluminum substrate, inspected by Champagne et al.[21] It demonstrates that between the deposited copper (the

light region) and the aluminum substrate (the darker region) forced mixing occurs, and that can only be attained by deep-impact infiltration of the copper particles into aluminum.

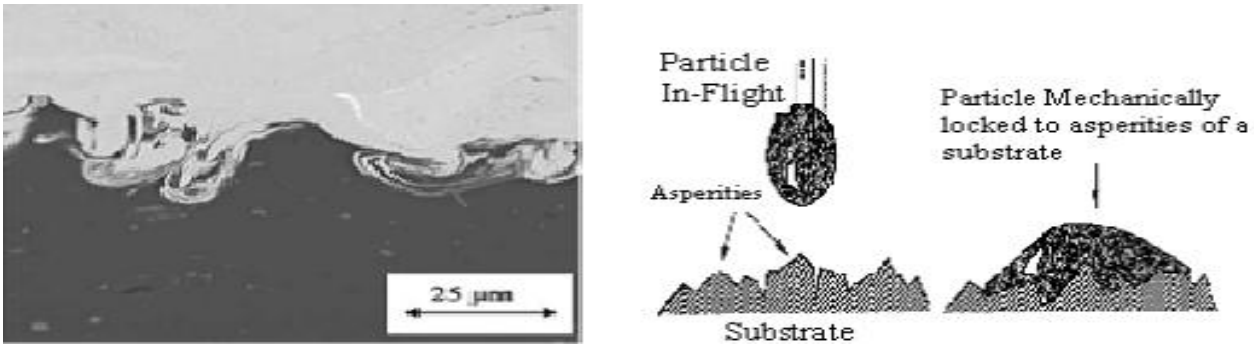

FIGURE 10 ENERGY DISPERSIVE SPECTROMETRY IMAGE OF COPPER COATING ON ALLUMINIUM [22] & MECHANISM OF LOCKING [23] IN COLD SPRAY

This model also elucidate the minimum particle velocity that is essential to achieve deposition. In order to deform the solid material plastically, a sufficient amount of kinetic energy is vital to be supplied and with the knowledge of adequate amount of kinetic energy, one can determine the minimum particle velocity required for coalescence. The empirical model devised by Champagne demonstrates that substrate coating interfacing depends upon the hardness of substrate and the density of coating material, solely with the velocity of particle (m/s) Vp required for the achievement of mixing at interfacial level.

$$Vp = [(7.5 \times 104)\ (B/\rho)]^{0.5}$$

Where B stands for the Brinell hardness number of substrate and ρ for the particle density (in kg/m^3).

1.3 INTRODUCTION TO REINFORCEMENT ELEMENTS

1.3.1 EPOXY RESINS [24, 25]

Epoxy resins or polyepoxides are reactive polymers which contain epoxide functional groups in their chemical structure. There are generally two types of epoxy resin reactions; first in which they reacts to themselves through catalytic homo polymerization and second in which they reacts with hardners like amines, acids, acid anhydrides, alcohols, phenols, and thiols to form long polymer chains. The cross-linking reaction caused by the addition of hardeners is generally termed as curing. The reaction of epoxy resins with themselves or with hardeners develops a thermosetting polymer. The thermosetting polymers are characterized by high chemical resistance, high temperature resistance, and high mechanical properties. Epoxy resins find their applications in metal coatings, in electronic and electrical component fabrication and insulation, high tension electrical insulators, fiber-reinforced structural plastic materials, and as structural adhesives.

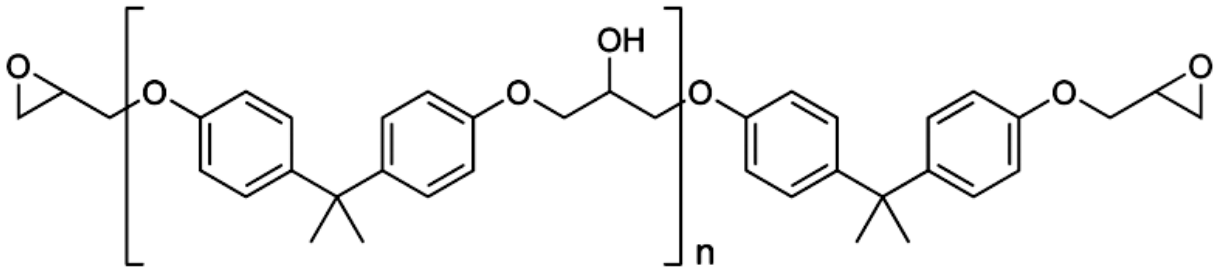

FIGURE 11 CHEMICAL STRUCTURE OF EPOXY RESIN

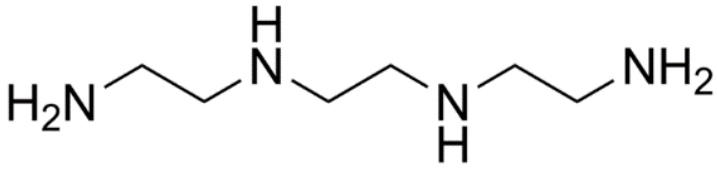

FIGURE 12 CHEMICAL STRUCTURE OF TRIETHYLENE TETRAMINE HARDENER

USE OF EPOXY RESINS IN DIE MAKING [26]

Since Epoxy resin is a thermoset plastic reinforced with composite material, it is characterized by certain mechanical properties such as strength, stiffness and hardness. It can be cast to desired shape before curing. It could easily be combined with the coating of cold spray to take shape of a permanent mold die. It is having a property of low shrinkage and high resistance to thermal expansion so ideally best for die support. It is capable of bearing high compressive loads.

Pulak M. Pandey et al [27] in his paper provides the brief overview idea of Rapid Prototyping technology, emphasizing on its ability to shorten the product design and development process. Also, this paper gives the brief idea about the different types of RP techniques along with the description of various stages of data preparation and model building. Factors of consideration before part deposition in RP technology can be inferred from the paper.

Chua et al [28] in their work, explains the manufacturing applications and the working principles of various Rapid Prototyping Techniques.

D.T. Pham et al [29] in their work, gives the detailed information about the construction and the working principle of Fused Deposition Modelling technique. Along with this, they explains the working conditions of FDM including the build material heating temperature and solidification and adhesion criterion. They also explains the motion control of the extruder nozzle as NC mechanism, in which the nozzle traces a tool-path which is controlled by a CAM software.

S. Au et al [30] in their work explains the necessity of consideration of the factors for achievement of a steady nozzle speed and material extrusion rate. They also explains the effects of the addition of support structure for overhanging parts, and the speed of the head over the layer thickness.

Chee Kai Chua et al [31] explains the whole process of FDM from CAD model conversion to physical production of the prototype including formation and removal of supports. They explains the beginning of FDM as a software process in which the CAD model of prototype is converted to Sliced Thin Layer (STL) format. They also explains the process of STL conversion as mathematical layering and orientation of the model for the purpose of building. About support structures, they tells that the support structures are generated within STL model and the machine dispenses multiple materials to achieve prototyping with support structures. They explains that the model is manufactured by extruding small blobs of thermoplastic material to produce layers as after extrusion from the nozzle, the material sets solid instantly. About motion and feeding they explains that the plastic filament or wire is pushed into the extruder nozzle typically by a worm-drive at a controlled rate and servo motors/stepper motors are deployed to relocate the extrusion head.

J. Karthikeyan et al [32] in his work explains the thermal spray process as advance material processing. In this work he explains the idea behind the process of thermal spraying. Also, a brief review of history of thermal spray processes has been discussed in the work.

V. K. Jr.Champagne et al [33] in their works explains the various types of thermal spraying along with the technologies that work behind each. They further explains the various parameters of the same that are taken into considerations. Their study also comprises the comparison of various thermal spray technologies.

Knight et al [34] in his work tells about the origination of very first thermal spray technology by Schoop. He explains how the notion grown from the model of a toy canon to a discovery that has changed the face of coatings in the world. He explains the contribution of Schoop in the development of various types of thermal spray technologies such as HVOF, Plasma and Cold Spray. He also tells about the applications of thermal spray such as wear and corrosion resistance marine and aerospace industry. He also explains the breakthrough that the technology has made in surface engineering.

Mitchell R. Dorfman et al [35] in his work, gives the idea about the technical and cost considerations for the selection of the type of thermal spray technology. He suggests that the technical considerations are relied on the understanding of the mechanism of wearing and the factors of environment, which the parts are exposed to. He also suggests that the cost contemplations include the equipment or process employed, the material employed, consumables like electricity and gas, cost of labor, and the component's life before it needs to be renovated. He explains the benefits of thermal spraying over other surface coating technologies as; lower cost, improved engineering performance, and/or increased component life which is associated with the technology. He also explains the applications of thermal spraying; in agriculture, papermaking and printing, computers, in aerospace, nuclear power, electronics, pumps/motors, geothermal, utilities involving sewage/water/power, defense, oil platforms, submersed pipe lines, railroad, automotive, and refineries.

H. Singh et al [36] in their work concisely labels the various facets of cold spray technology, also explaining the crucial parameters that affects the deposition conduct along with pros and cons; applications and history of advent of cold spraying. They have concluded cold spray technology as an emerging technology to enhance and enlarge the series of uses for thermal spray procedures as a greener auxiliary according to stringent environmental and health safety regulations rather not for the replacement of any of the deep-rooted coating methods. They also frames the future scopes of the study of the technology as designing of optimum parameters like nozzle design, temperature control, nature of gas, and its material and also estimate of critical velocity for different substrate and particle blends.

J. Pattison et al [37] reports on the progress of a fresh freeform construction technique using cold spray. They also reports that the process is capable of producing functional forms by employment of unique manufacturing strategies for cold spray. The paper gives statistics on the process including details of tactics incorporated during the fabrication of the component. They concludes the possibility for building the components from materials like Ti, which unveiled embedded devices, internal channels and freeform surfaces.

T. Stoltenhoff et al [38] in their work gives the analysis of cold spray process as an outcome of CFD analysis and wide-ranging spray experiments. In their experiments, they modeled particle and the gas flow field for different geometries of nozzle and parameters of the process in association with the experimental results. They find that when the powder particles surpass a critical impact velocity, adhesion occurs, that is explicit to the material. For spherical powder of Cu with slight O_2 content, they reported that the critical velocity was about 570 m/s. Using nitrogen as the process gas and 5-25 μm particle grain sizes, they reported deposition competences of above 70%. They also reported that the coatings made by cold spray show insignificant porosity and O_2 contents akin to the primary feedstock powder.

S. Grigoriev et al [39] in their work explains the fundamentals of the process with the mechanism of coating. They also gives the empirical relations associated with the process. Further they explains the construction of the apparatus and the comparison of cold spray with other thermal spraying technologies.

OH. Fukanuma, R.Z Huang et al [40] studies Aluminum, Nickel, and Copper coatings deposition by Cold Spray on three different of substrates, copper, aluminum and Steel. They tested the hardness of the substrates and the tensile strength of the coatings. They also reported the influences of substrate hardness on the tensile strength of the coating. They also discussed the influences of working gas temperature on the tensile strength.

Shuo Yin et al [41] investigates the effect of spray angle on the distribution of temperature within the metal substrate in the process of cold spray. They employed CFD approach in the work to accomplish the objective. Their simulation results displays that spray angle considerably influences the temperature distribution within the substrate. They concludes that for the perpendicular spraying, the temperature gradient contours present frequently annular shape, which means the temperature distribution is only reliant on the radial position. Furthermore, they reports that the topmost value of the surface temperature is not at the geometric center (stagnation point) but at the position slight away from the center, which may result from the evolution of the flow from laminar to turbulent

state. They finds that the best way to preheat the substrate at the angular condition is to move the nozzle from uphill toward the downhill direction.

Hyun-Boo Jung et al [42] conducted **t**rials on the length ratio and the expansion ratio of the nozzle, in terms of their relation to the temperature, gas pressure, and length of nozzle, to reduce the shockwave**.** They reported that when the convergent length is increased, the particle temperature upsurges and the particle velocity reduces. When the divergent length is increased, the particle velocity increases and the particle temperature drops. When the expansion ratio of the nozzle is 4.27, the velocity of particle touches an extreme of 633.1 m/s and the shock wave is minimized. The optimal ratio of expansion for the nozzle increases with increases in the nozzle length and gas pressure. With change in gas temperature, there is no change in the optimal expansion ratio of the nozzle.

K. Sakaki Y. Shimizu et al [43] in their study, di numerical simulation and experiments to scrutinize the consequence of the geometry of entrance for the nozzle. They reported that the gas flows subsonic in the convergent section at the entrance of the nozzle and it exhibit a relatively higher temperature. The convergent section at the entrance thus, is best suitable for heating spray particles. They also reported that the change in entrance convergent section length of the gun nozzle had a significant effect on the microstructure, hardness and deposition efficiency. As the entrance geometry is increased, the deposition efficiency and hardness also increases.

S. Yin et al [44] investigated the effect of injection gas pressure on particle acceleration, dispersion and deposition in cold spray process by both numerical and experimental methods. They developed a computational fluid dynamics (CFD) model which exactly matches the real nozzle in experiment to predict the supersonic gas flow field and particle velocity prior to the impact. Based on the simulation results, they found that injection pressure expressively disturbs the flow field of the driving gas. Higher the injection pressure, higher is the injection flow rate as well as powder injection rate, producing thicker coating on the substrate. Besides, they compared the anticipated particle footprints on the substrate surface at different injection pressures with the experimental measurements of the solitary track coating width and found that particles scatter more broadly at higher injection pressure.

Hiroshi KATANODA et al [45] experimentally investigated the internal flows in the cold spray nozzle including shock waves. In their apparatus, the nozzle consisted of the diverging section with the design Mach number of 2.0, followed by a straight passage, a barrel, with the length of ten times as much as its equivalent diameter. The compressed dry-air was used as a working gas. The wall

static pressures of the nozzle were measured and internal flows of the barrel were envisaged. The internal flows were also analyzed by assuming the shock wave in the barrel to be the normal shock wave and pseudo-shock wave. They reported that when the shock wave in the barrel was assumed to be the normal shock wave, calculated pressure ratios for the particular location of the shock wave were largely diverse from the experimental data. Whereas, when assuming the shock wave in the barrel to be the pseudo-shock wave the calculated pressure ratios versus the sites of the first shock wave harmonize well with the experimental results.

C.-J. Li et al [46] reported that the critical velocity depends not only on materials types, but also on particle temperature and oxidation conditions. They changed the oxygen content in the powders by isothermal oxidation at ambient atmosphere. They examined the effect of oxygen content on the critical velocity and reported that the critical velocity in cold spray was ominously swayed by particle oxidation condition in addition to materials properties. They reported that the critical velocity of copper particles altered from about 300 m/s to over 610 m/s with the change of oxygen content in powder. They found that the materials properties influenced the critical velocity more notable at low oxygen content than at high oxygen content. Their results suggest that with a rigorously oxidized powder the critical velocity tends to be dominated by oxide on the powder surface rather than materials properties.

A. Sova et al [47] studied numerically the influence of powder preheating on the particle impact by considering two cases with powder injection to subsonic and supersonic regions of the nozzle. They reported that the artificially preheated 10–50 μm copper particles axially injected to the supersonic region of the nozzle had higher influence temperature than the particles injected to the nozzle pre-chamber. They explained this effect by the dependence of duration and intensity of gas–particle heat exchange on the location of powder injection point. They also reported that in the case of powder injection to supersonic zone, the application of powder preheating could shift the particle impact parameters towards the deposition window without increasing the working gas stagnation temperature.

A. Moridi et al [48] studied single and multi-pass deposition of a 0.5 mm thick Al 6082 coating on the same substrate to explore the number of passes effect on mechanical characteristics. In addition, they investigated one pass deposition of 0.65 and 0.8 mm thick coating is investigated to examine the thickness effect. They performed micro-structural observation, micro-hardness measurements and X-Ray diffraction (XRD) measurement of residual stress on all groups. They also carried adhesion test and tubular coating tensile test to characterize the coating in different cases. They used

the observation of fractured surface to investigate the failure mechanism of the cold-sprayed coating. They reported that increasing coating thickness led to a progressive release of the residual stress at the interface between coating and substrate. Less compressive residual at the interface was obtained for the thickest coating. They also reported that increasing coating thickness resulted in decreasing both the compressive stress state at the interface and bond strength and the number of passes didn't have a substantial effect on bond strength of the coating. Further, they found that in two pass deposition the cohesion strength decreased in comparison to the single deposition method and increasing the number of passes from two to three resulted in an increase of cohesion strength. Furthermore, they reported that by increasing the number of passes, the mixed mode fracture becomes present in the outer layer of the coating since in a subsequent number of passes there are pores and infirm particles which act as pre cracks.

Xian-Jin Ning et al [49] established a 2-D model of the low-pressure cold spray with a radial powder feeding using CFD software in their study. They simulated the flow field for both propellant gases of nitrogen and helium. To predict the in-flight particle velocity and temperature, they introduced a discrete phase model to simulate the interaction of particle and the supersonic gas jet. They used the experimental velocity of copper powder with different sizes to validate the calculated one for low-pressure cold spray process. Their results show that the computational model can provide a satisfactory prediction of the supersonic gas flow. They found that similar velocity was obtained with the drag coefficient formula of Henderson and with that of Morsi and Alexander. As the shape factor was estimated, the reasonable prediction of velocity for non-spherical particle can be obtained, to compare with the experimental results.

Huang Guoshenga et al [50] reports that instead of injected by high pressure powder feeder, powders can be drawn into the nozzle by syphonage effect generated by supersonic gas flow in low pressure cold spray which makes low pressure cold spray convenient for on-site operation. In their study, a CFD software (STAR CCM+) was used to calculate the gas flow in nozzle of the DYMET 413 commercial low pressure cold spray system. Also the variation of structures and process parameters based on the commercial system were also investigated. They reported that the syphonage effect is strongly influenced by the powder feeding location, the temperature and pressure in prechamber has little effect on syphonage effect in powder feeder pipe. The syphonaged gas decelerates the gas velocity and low down the gas temperature in nozzle, so it was found best to control the mass flow rate of powder feeding gas by selecting the location. They also reported the

disadvantages that the particles in syphonage system collides with the nozzle wall which makes the nozzle a short service life.

Zhenhua Cai et al [51] investigated the relationship between the coating profile and the spray distance. In this work, a method for simulating coating profile was applied; 2D coating profile was fitted as Gaussian curve in Matlab. The relationships between spray distance, scanning step, and coating thickness, deposition efficiency were described.

R. Huang and H. Fukanuma et al [52] studied the Influence of Particle Velocity on Adhesive Strength of Cold Spray Deposits. They reported that the in-flight particle velocity was increased with the increase of gas pressure and temperature or using helium instead of nitrogen gas. Similarly to the particle velocity, the adhesive strength of coatings to the substrates increased too with the increase of gas pressure and temperature or using helium instead of nitrogen gas. They also noticed that the particle velocity plays an important role in improving adhesive strength based on plastic deformation. A higher particle velocity benefits the mechanical interlock effect resulting in excellent bonding between the coating and substrate.

Xinkun Suo et al [53] studied strong effect of carrier gas species on particle velocity during cold spray processes. They developed a computational fluid dynamics (CFD) model to predict the gas flow and particle velocity both inside and outside the nozzle. They validated the model experimentally. It was reported that the carrier gas species was an important factor of the particle velocity. For an air propellant gas, using helium as the carrier gas increased the particle velocity due to the low average molar mass of the mixed propellant gas. Similarly, increasing the helium carrier gas pressure increased the molar fraction of helium in the mixed propellant gas and, thus, the particle velocity.

Wen-Ya Li and Chang-Jiu Li et al [54] conducted numerical analysis for the accelerating behavior of spray particles in cold spraying using a computational fluid dynamics program, FLUENT. They achieved the optimal design of the spray gun nozzle based on simulation results to solve the problem of coating for the limited inner wall of a small cylinder or pipe. They reported that the nozzle expansion ratio, particle size, accelerating gas type, operating pressure, and temperature were main factors influencing the accelerating behavior of spray particles in a limited space. They confirmed the feasibility of optimal design for a spray gun nozzle by experimental results using the designed short nozzle with a whole gun length of <70 mm.

Hezhou Ye et al. [57] in their research have found that the deposition of the Al on the polycarbonate material is effectively possible by cold spray technique. The polycarbonate material like Lexan have strong resistance to impact and abrasion, high tensile strength and low density. This features makes it widely used thermoplastic polymer and utilized in nuclear field, medical and aerospace but have poor electrical conductivity. To enhance its electrical conductivity, high temperature operation and erosion resistance metallization with the Al coating is required but have poor surface modification properties by the conventional coating processes. Thus cold spray is introduced for it. They have found the powder feeding rate be the dominant component for effective results at the maintained pressure and temperature. This study first time demonstrate the metallic coating on any polycarbonate material.

Maurice J.A.A. Goris et al. [58] in their research papers have found that the electrical conductive foils can be made cheaper without disturbing its conductivity by cold spray coating of the copper on the aluminum sheets. The experiment have concluded that the layers of Al sheet then Cu powder being cold sprayed and then conductive adhesive joins another cold sprayed Al sheet with Cu surface having contact via adhesives which are conductive. The primary aim of their experiments is to make the available sheet cheaper with same electrical conductivity. They have achieved the cheaper product on scale of 10 but there is degradation of the copper layer till first 200 cycles of the operation but after than it become stable while Al sheet without cold sprayed with Cu seems to have 400 cycles degradation decreasing in a linear form. Thus the degradation is removed up to appropriate level by their experiments.

Narinder Kaur et al [59] in their research have found that the Thermal spray coating of the corrosion-erosion resistant Cr and Ni on the boilers steel tubes which was done earlier for resistance of corrosion and erosion at high temperature have some oxidation and chemical behavior different than estimated. They have taken boiler steel tube material of power plants i.e. T22 and SA516 which are polished then grit blasted to have rough surface and proper material interlocking with powders and used the powder for cold spray as mixture of micro and nano sized Ni and nano sized Cr termed as Ni-20Cr. The nano particle seems to be more effective in coating using square exit DeLaval nozzle than the micro particles due to less density and high resistance to corrosion and erosion.. The adhesion strength, scratch resistance and indentation are found using high tech devices like Ducom, TR-101 etc. The oxidation process is performed by washing the specimen with acetone. The results shows that oxidation of the powder do not take place using XRD/SEM/EDS techniques. Due to introduction of the nano particles in the cold spray along with micro particles the hardness and the

erosion-corrosion resistance than the bare boiler steel tubes. Thus cold spray utilized to improve its material quality even at elevated temperature after CS process is being done.

A.Sova et al. [60] in their research have found the effect of the powder feedstock entry position into the cold spray apparatus that can lead to maximum deposition efficiency. They found that powder entered after throat of nozzle and mix with pre heated air have more deposition efficiency than entering it before the throat thus reducing the efficiency and increasing wear and tear of the nozzle because it not only depend on impact velocity but also on impact temperature during coating. Thus injection of the Cu powders in supersonic region after the throat in DeLaval nozzle lead to impact velocity and temperature even in low working gas temperature and more sensitive to thermal advantage of preheat air than if enters in nozzle in sub sonic region i.e. before throat, in this case all favoring parameters will not be effective at all.

Michael Saleh at al. [61] in their research have found the effect of the single particle and multi particle strike on the substrate and its dependence on temperature and residual stress. In this study they also present measurements of residual stress in macroscopically thick AA-6061-T6 CS coatings, 3–4 mm thickness, produced using two slightly different spraying techniques. The experimentally determined through thickness stress profiles by neutron diffraction on macroscopically thick coatings were used to validate FE calculations made for 100 μm thick coatings. The local temporal temperature can exceed the melting point of aluminum in areas of particle–substrate contact. The increase in temperature is essentially linked to the loss of shear strength leading to the various properties changes through the thickness in the sprayed layer in CS technology. The residual stress was calculated via MATLAB also and significant plastic strain gradient is observed in the through thickness of the cladding material and within each particle. The large degree of deformation is closely linked to the non-uniform temperature distribution and thermal softening behavior. More strain was observed in lower sprayed length than upper. The results can be summarized as initial primary particle deposition with adiabatic shear instabilities forming in the jetting region with further plastic deformation upon impact by secondary particles, adiabatic plastic deformation of secondary particles with larger elongated grains and isothermal heating of the specimens induced by the successive impact of secondary, tertiary and quaternary coming sprayed particles.

T. Hussain et al. [62] in their research have found the contribution of the bonding mechanism in the cold spray technique by the comparison of the metallurgical bonding(Substrate + Particle) and mechanical interlocking(particle + sprayed layers with the methodology of using a short heat treatment to promote inter diffusion and intermetallic formation. The Micro-pores and defects were

found in the grit blasted surface resulting low bond strength. The substrate surface roughness has an effect only on the first few layers of coating deposited, and thus the effect on deposition efficiency may be small. In their experiment they perform CS using DeLaval nozzle, Cu pwoder on Al polished and grit blasted, polished and ground substrate and did the bond strength and fracture testing. The bond strength is higher if CS is done on Grit blasted substrate which is annealed prior to CS.

V. Lemiale et al. [63] in their research have described the model which shows combine effect of the strain rate and the temperature as a 3D model as a single Cu particle impacting the Cu substrate using smoothed particle hydrodynamics. The assumption of both particle and substrate at room temperature initially during the impact and using low strain rates are incorrect and provide misleading results because thermal softening can change final attributes of the CS coating. This experiment leads to optimize the process based on data that are not available in experimental setups and will allow investigating fundamental aspects in the physical mechanisms of cold spray.

Renzhong Huang et al. [64] in their research have developed the ultra-strong bonding between the particle and the substrate and its measurement is done by pull test and corresponding stress and strain graphs are plotted, effect of critical velocity and splat formation effected by impact temperature. The initial applied impact by the powders was used to initiate the jet formation in substrate that will lead to CS coating in effective way.

J. Cizek et al. [65] in their research have used four blends of Al powder containing different amounts of Ti using low-pressure cold spray were deposited onto Ti–46Al–7Nb substrates as oxidation protection layers. The coating morphology and chemical composition were assessed. Optimized heat treatment in protective atmosphere was carried out in order to induce formation of intermetallic phases within the deposits and the specimens were then subjected to 950 °C exposure for 100, 250, and 500 h and their oxidation performance was monitored using the gravimetric method and reduction in the oxidation rate was observed. The oxidation rate of the specimens is significantly reduced by a deposition of cold sprayed Al + Ti coatings, probably due to the easier formation of Al2O3 scale due to the added Al and execss of Ti in coating inhibits Al2O3 passive layers.

J. Henao et al. [66] in their research have found the effects of the process conditions such as spraying distance, gas pressure and temperature on the microstructure of Fe-based amorphous sprayed coatings on mild steel substrate. They explained how the dense coating can be done with porosity below 5%.and efficiency decreases at higher gas pressure. Particles during the impact undergo a shear rate of 107–109 s-1.The efficiency of the coating decreases as the stand-off distance between the nozzle and the substrate increases. The temperature studies shows that efficiency and properties

of coatings were poorer when the spraying gas temperature was higher (1000°C). The hardness value also decreased due to high temperature, pressure and standoff distance leading to less denser microstructure and more porosity but results are good when the conditions are optimal.

M. Gardon et al. [67] in their research they have Cold Gas Spray (CGS) titanium/hydroxyapatite coatings were deposited onto Ti6Al4V by means of different feedstock blends of metallic and ceramic powder with the aim of building-upwell-bonded homogeneous coatings. Coatings were immersed in Hank's solution for 1, 4 and 7 days, bonding strength value was above 60 MPa even after 7 days, which improves the results obtained from conventional thermal spray technologies. This process depends upon the % of particle size and diameter ratios. 30 vol. % of the blend was HAP and 70 vol. % titanium and the particle diameter ratio of HAP: Ti was 1:2. Thus blending certain percentages and particle diameter ratios of plastically deformable Ti powder and non-deformable HAP leads to excellent mechanical and biological properties.

Edward Joshua T. Pialago et al. [68] in their research had cold sprayed Copper (Cu)-carbon nanotube (CNT) composite powders with CNT 15%. The Mechanical alloying (MA) powder and CS coating samples were characterized by weight and size measurements, optical microscopy, scanning electron microscopy, energy-dispersive X-ray spectroscopy, and X-ray diffraction. The increase of CNT content resulted to the reduction of the particle size of the MA composite powders. Also, the DE of the composite powders decreased with the increase of CNT content as well as with the increase of the number of coating layers. The composite coating has lamellar structure but internal pores as well. The coatings with10 vol. % CNT had more pores than the other coatings. The surfaces of the composite coatings had compacted and flattened plateau-like features and crater-like formations. These were likely due to the peening and grit blasting effects that resulted from the rebounding of particles as indicated by the low DE of the composite powders. The XRD results indicated that the composite powders and coatings had micro strains and had undergone grain size reduction due to the deformation caused by MA and CS techniques. The roughness values tended to decrease with the decrease of particle size. The surfaces of the coatings contained about 1.0–2.5 vol. % micro pores.

Sukhminderbir Singh Kalsi et al. [69] in their research did NiCoCrAlY coating on Superfer 800H super alloy with cold spray process to reduce the degradation rate of substrate super alloy in actual medical waste incineration environment and in chlorine based environment operating at high temperature. The wear erosion and corrosion performance of uncoated and cold sprayed super alloy was evaluated in the secondary chamber of medical waste incinerator. The degradation rate of the

specimens was assessed by measuring the thickness loss of the specimen after cyclic exposure for 1000 h in medical waste incineration environment. The active oxidation in presence of chlorine and formation of porous, fragile and non-protective scale of Fe2O3 lead to poor performance of the uncoated super alloy substrate surface. Degradation rate of uncoated super alloy is 157.95 mpy which is quite larger than degradation rate of 36.56 mpy for NiCoCrAlY coating in medical waste incineration environment. Due to the formation of Al2O3 with some spinels of Co–Cr and Ni–Cr at top of scale and dense structure of coating.

Gobinda C. Saha et al. [70] in their research present work on two feedstock powders, namely nano-crystalline and microcrystalline WC-Co cermets, with identical matrix phase content: WC-17wt. %Co. An engineered duplex Co coated WC- 17wt.%Co cermet particle designed to withstand coating spalling under elevated loads as well as to limit abrasive debridement during the wear is introduced for the first time to produce a more homogeneously-dispersed coating microstructure. WC-Co cermet system offer better wear resistance and greater flexibility in applications. CS deposited coatings of the nano-crystalline and microcrystalline powders were examined for micro hardness, fracture toughness, sliding abrasion (ASTM G133-05) and dry-sand rubber wheel abrasion (ASTM G65-04) wear performance. It was found that the wear rate increased with increasing applied loads, while it decreased with increasing sliding distances. The decarburization of the coating using the novel nano-crystalline powder was significantly lower when compared with the micro structured coating of same composition. The mechanical and tribological behavior of the optimized nanostructured coating generally overcome those of conventional micro structured coating of similar composition (WC-17wt.%Co) by increase in micro hardness, fracture toughness, and wear resistance.

A.Moridi et al. [71] in their research found the effect of single and multi-pass deposition of a 0.5 mm thick Al 6082 coating on the same substrate is studied to explore the number of passes effect on mechanical characteristics. Micro-structural observation, micro-hardness measurements and X-Ray diffraction (XRD) measurement of residual stress were performed and the increased coating thickness led to a progressive release of the residual stress, decreasing the compressive stress state at the interface and decrease bond strength the interface between coating and substrate, decrease cohesive strength between the powders and number of passes had an insignificant effect on the residual stress, bond strength, increase cohesion strength.

N. S. Cheruvu et al. [72] in their research did long-term isothermal tests on the thermal barrier-coated (TBC) specimens at three temperatures 1010°C (1850°F), 1038°C (1900°F), and 1066°C

(1950°F) to determine the effects of long term exposure on the TBC failure location (mode). The isothermal testing, the samples were destructively examined to characterize the degradation of the TBC and determine the extent of thermal grown oxide (TGO) cracking, TGO growth, bond coat oxidation, and TBC failure location after long term exposure for up to 18,000 h. Optical microscopy and a scanning electron microscope (SEM) attached with an energy dispersive spectroscopy (EDS) system were used to study the degradation of the TBC and bond coatings. The results showed that long term isothermal exposure leads to a change in the TBC failure mode from the delamination of the TBC at the TGO/TBC interface to the internal oxidation of the bond coat and bond coat delamination. Isothermal testing performed on TBC-CoNiCrAlY-coated GTD-111 specimens showed that the presence of the TBC accelerated the kinetics of TGO formation, formation of mixed or transient oxides and bond coat degradation. The extent and size of the cracking increased with the exposure temperature and time. Internal oxidation directly proportional to time and temperature exposure. The responsible factor for the delamination of the bond coat after long-term thermal exposure is the coalescence of Kirkendall voids at the interface.

3.1 OBJECTIVE

The prime objective of this research study is to device a new technology to fabricate complex plastic injection molding permanent dies in an easy and economical manner. The major objective is although divided into various milestones mentioned afterwards:-

- ✓ Design of Cold spray apparatus.
- ✓ Fabrication of Cold spray apparatus.
- ✓ Validation of the fabricated system by depositing thick metal layers over the workpiece.
- ✓ Optimization of the spray parameters and workpiece conditions as per the final product.
- ✓ Fabrication of permanent mold employing the stated research.

3.2 SCOPE OF STUDY

Presently the permanent molds for plastic and metal casting are made by metal removal processes such as milling which consume a lot of time and capital resources. If the design of the product is a bit more complex it further adds up to the time as well as the cost incurred in making the molds. This directly affects the price of consumer product. The advanced technology is not only the one which produces something in a new way but which makes something in new as well as efficient way. This research has the potential to make a breakthrough in the mold making technologies. The method to be undertaken in the said research involves the development of such a technique which is cheap, easy and virtually independent of the complexity of the part shape.

3.3 HYPOTHESIS

Deposition of thick layer (>1mm) of metal (copper) over Fused Deposition Modelled full scale copper electroplated and bare ABS pattern by employing fabricated Gas Dynamics Cold Spray apparatus to form mold.

3.4 METHODOLOGY

The experimental procedure undertaken during the research study to validate above hypothesis is as follows:-

PHASE-I

- Selection and design of the workpiece.
- Preparation of CAD model of pattern and conversion to Sliced Thin Layer format.
- Printing of full scaled model in three dimensional coordinates using Fused Deposition Modelling.

- Surface finishing of the pattern.
- Preparation of two types of samples viz. raw ABS and copper electroplated patterns.

PHASE-II

- Design and simulation of cold spray apparatus.
- Fabrication of optimal apparatus.
- Trial for deposition of thick copper metal layers on both the samples by spraying, to check feasibility.

PHASE-III

- Experimentation on certain number of specimen under different parameters.
- Evaluating deposition thickness, surface roughness and hardness of the samples.
- Optimizing the values for spray parameters and workpiece preparation.
- Preparation of job over optimized parameters.
- Sintering and extraction of molds.
- Reinforcement of molds and their finishing.
- Subjecting to practical application such as plastic injection molding or straight away plastic casting.
- Inference evaluation.

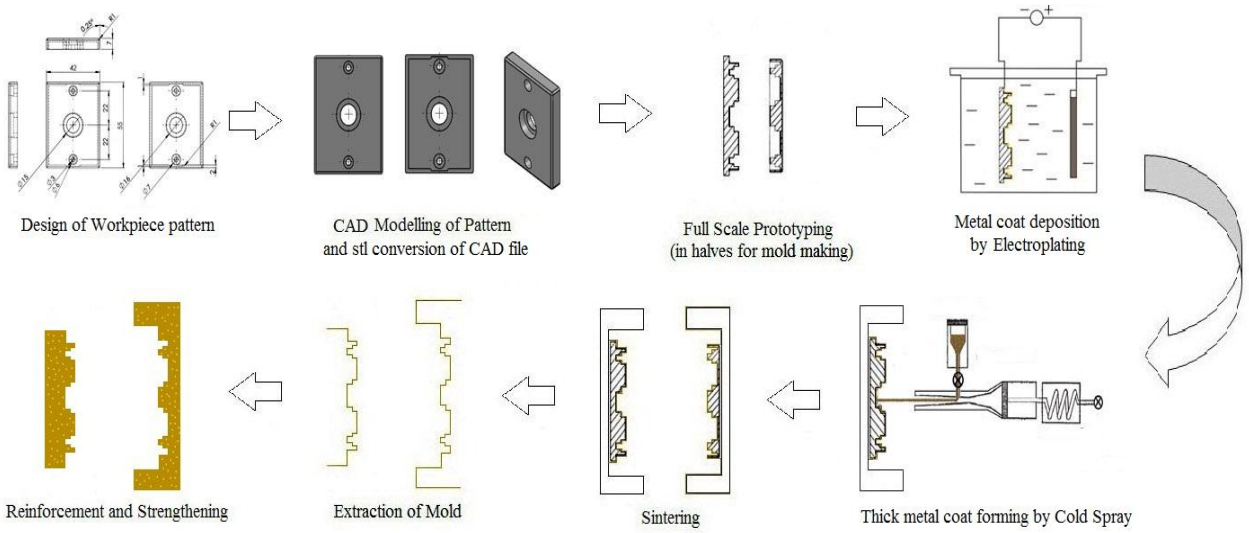

FIGURE 13 FLOW CHART SHOWING METHODOLOGY

3.4.1 RESEARCH METHODOLOGY

Experimental Design and Analysis using Taguchi method

Taguchi method rationalizes and standardize the fractional design. In this method, orthogonal arrays are built to design the experiments. It also proposes a standard method for result analysis. These orthogonal arrays are indiscriminate Graeco-Latin squares. Any two columns of an orthogonal array is found to be making a 2-factor complete factorial design. Which means that, whatever that does happens to all the other parameters at one level of parameter being studied also happens in the same way at other levels being studied. The effect of one parameter under study is separable from the effects of other parameters. Thus the combination and optimum level of each factor can be determined. The second feature is that, orthogonal array minimize the number of experiments. A factorial trial with 3 parameters each at 6 levels would require ($3^6 = 729$) test runs, whereas Taguchi L9 orthogonal array would require only 9 trial runs for framing the same information. In the Taguchi method, the results of the experiments are analyzed to accomplish one or more of the objectives that follows under:

Establishment of the best and/or the optimum conditions for a process.

Estimation of the influence of individual variables and their interactions with the process.

Estimation of the responses under optimal conditions.

The prime conditions are recognized by studying the core effect of each of the parameters. The core effects indicate the common tendency of effect of each parameter. The acquaintance of the influence of individual parameter plays a vital role in determining the nature of control to be established on a process.

3.4.2 WORK PROCEEDINGS

DESIGN OF APPARATUS

❖ NOZZLE

In the converging part the diameter is reducing linearly till throat from 8 mm to 2mm (10 mm long) while afterwards from throat to diverging section end it is increasing from 2 mm to 5 mm (40 mm long). As per the optimal attributes of design [55], the stated dimensions (shown in figure 14) were taken and performed fluid flow simulation (shown in figure 15) upon, applying the optimal boundary conditions (temperature=500°C, pressure=1000000Pa) [56] for low pressure cold spray system. The flow simulation yielded that a velocity of 875.628m/s can be achieved on the parameters.

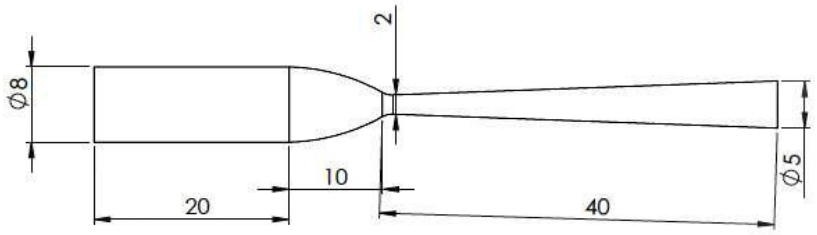

FIGURE 14 SKETCH SHOWING OPTIMAL PARAMETERS OF DE-LAVAL NOZZLE CORE

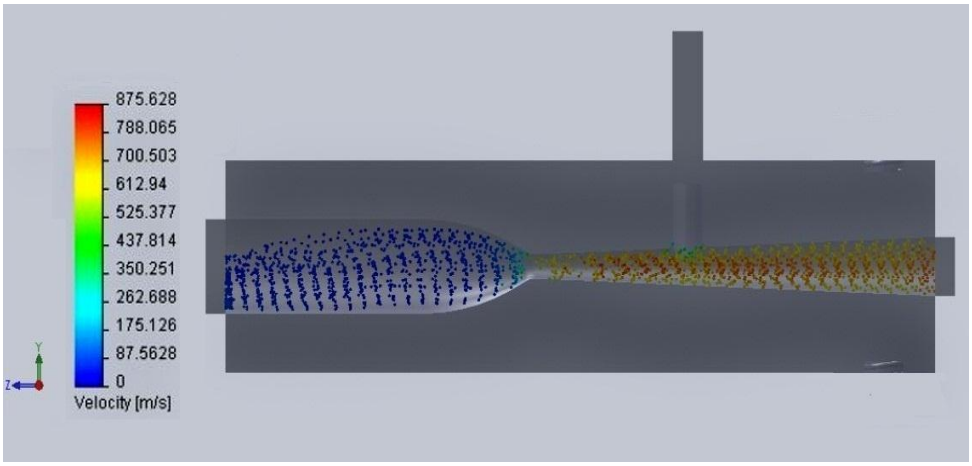

FIGURE 15 FLUID FLOW SIMULATION OF DE-LAVAL NOZZLE PERFORMED IN SOLID WORKS®

❖ GAS HEATER

The heater is designed in such a way that it heats the pressurized air up to 600°C and its purpose of heating is such that it should make the air more aerodynamic, less denser and light weight so that it perform its task of carrying the metal powders effectively, without melting them. The required length of articulated ceramic body, for the achievement of the said goals was estimated to be 12 inches. Figure 16 shows the CAD model of the gas heater.

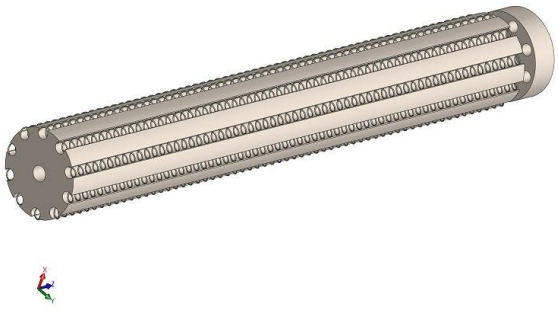

FIGURE 16 CAD MODEL OF GAS HEATER

❖ GUN CASING AND MOUNTINGS

Austenitic stainless steel 304 (18% chromium and 8% nickel) was found most relevant for the application as it has capability to withstand elevated temperatures up to 700°C and its own melting point is 1450°C. The casing was designed 14 inches long tube with 3mm thickness. The flanges and other mountings are designed of the same configurations. Figure 17 shows the CAD model of casing and different mountings of cold spray gun whereas figure 18 the CAD models of complete assembly.

FIGURE 17 CAD MODELS OF GUN CASING AND MOUNTINGS

FIGURE 18 CAD MODELS OF COMPLETE ASSEMBLY

In order to determine wholesome aerodynamic performance of the gun, fluid flow simulations were made on the assembly which are shown in the figures 19 and 20. The boundary conditions were taken as temperature=500°C, pressure=1000000Pa. The flow simulation yielded that there is velocity drop in the assembly and a final velocity of 625.066m/s can be achieved on the parameters.

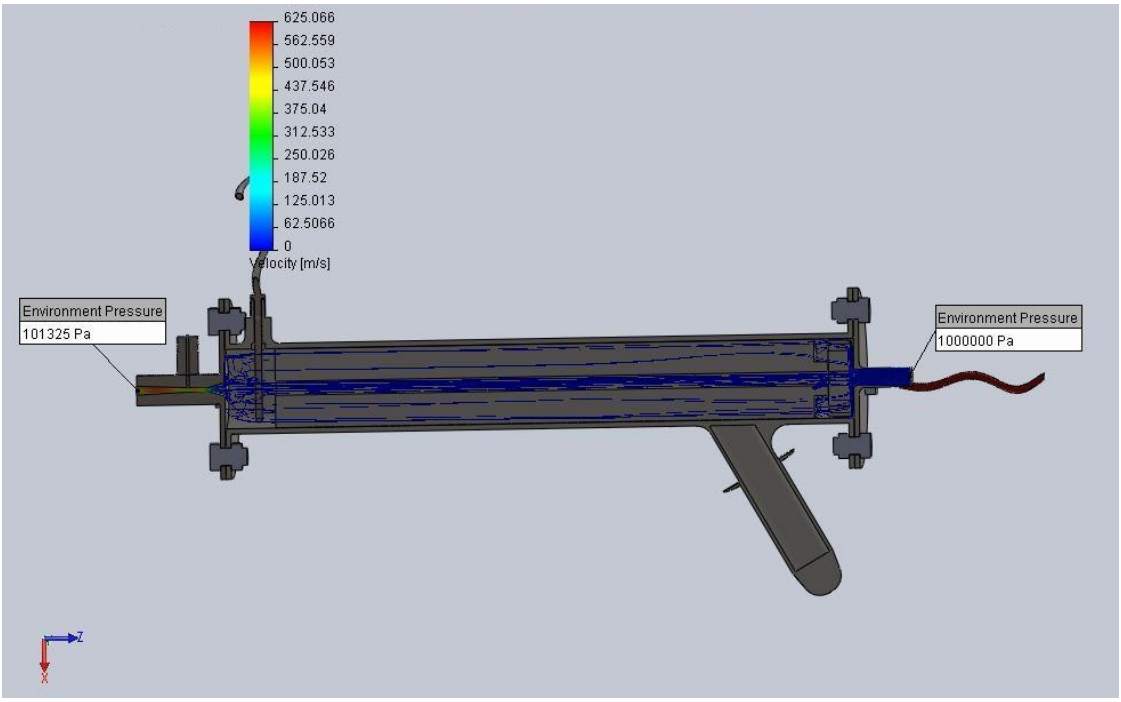

FIGURE 19 FLUID FLOW SIMULATION ON GUN ASSEMBLY

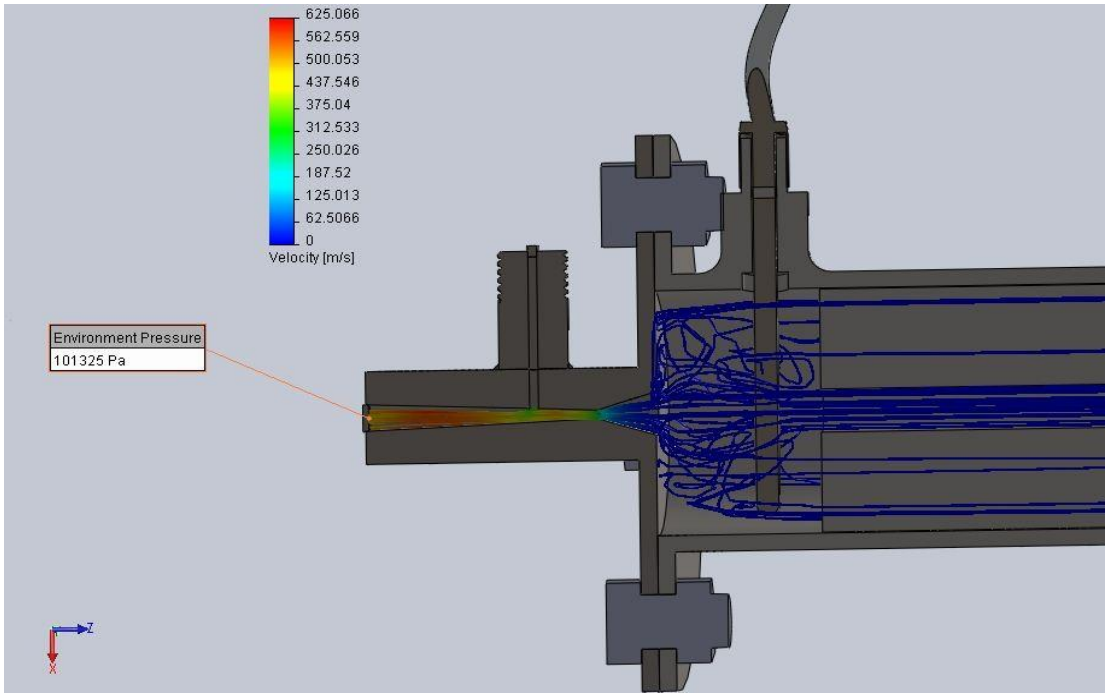

FIGURE 20 FLUID FLOW SIMULATION ON NOZZLE AND GUN ASSEMBLY

❖ MACHINING TOOLS

Since the nozzle's inner cross-section is intricate and a high accuracy is desired to meet the application needs, Electro-Discharge Machining (EDM) was found most appropriate and most economical. The tool for EDM were designed so as to be turned on a CNC lathe to achieve higher levels of accuracy.

FIGURE 21 CAD MODELS SHOWING THE NOZZLE AND THE EDM TOOLING DESIGN

FABRICATION OF APPARATUS

The fabrication process started with the CNC turning of EDM tools, figure 22 shows the photographs of the turned tools.

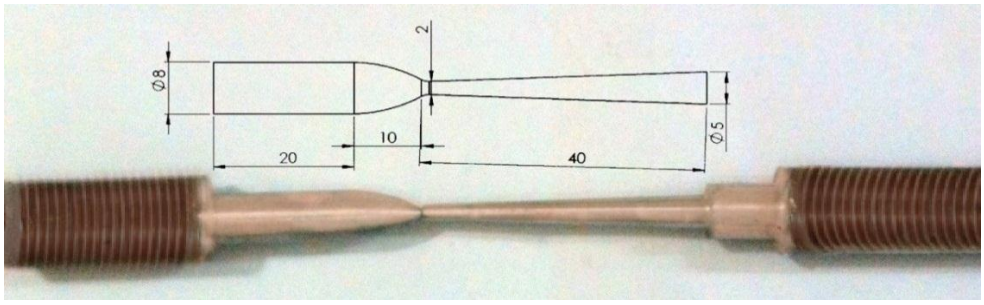

FIGURE 22 PHOTOGRAPH OF TOOLS FOR ELECTRO-DISCHARGE MACHINING OF DE-LAVAL NOZZLE

Performing Electro-Discharge Machining over the straightened EN-38 die steel billet having hole drilled through it led the manufacturing of the nozzle. The nozzle was subjected to induction

hardening for improving the abrasion resistance. Figure 23 shows the photograph of manufactured De-Laval nozzle.

FIGURE 23 PHOTOGRAPH OF MANUFACTURED DE-LAVAL NOZZLE.

Next to the nozzle, heater fabrication was done. The heating elements are axially fixed at the through holes on the periphery of the nozzle surrounded by the ceramic insulators, having electrical terminal at the end.

FIGURE 24 PHOTOGRAPH OF MANUFACTURED GAS HEATER

After having the gas heater built, gun casing and mountings were manufactured from procured stainless steel flats and tube which were put altogether by performing Gas Tungsten Arc Welding (GTAW). Figure 25 shows the photograph of gun casing and mountings.

FIGURE 25 PHOTOGRAPH OF GUN CASING AND MOUNTINGS

Figure 25 shows the labeled photograph of the complete cold spray system along with the control and feed elements.

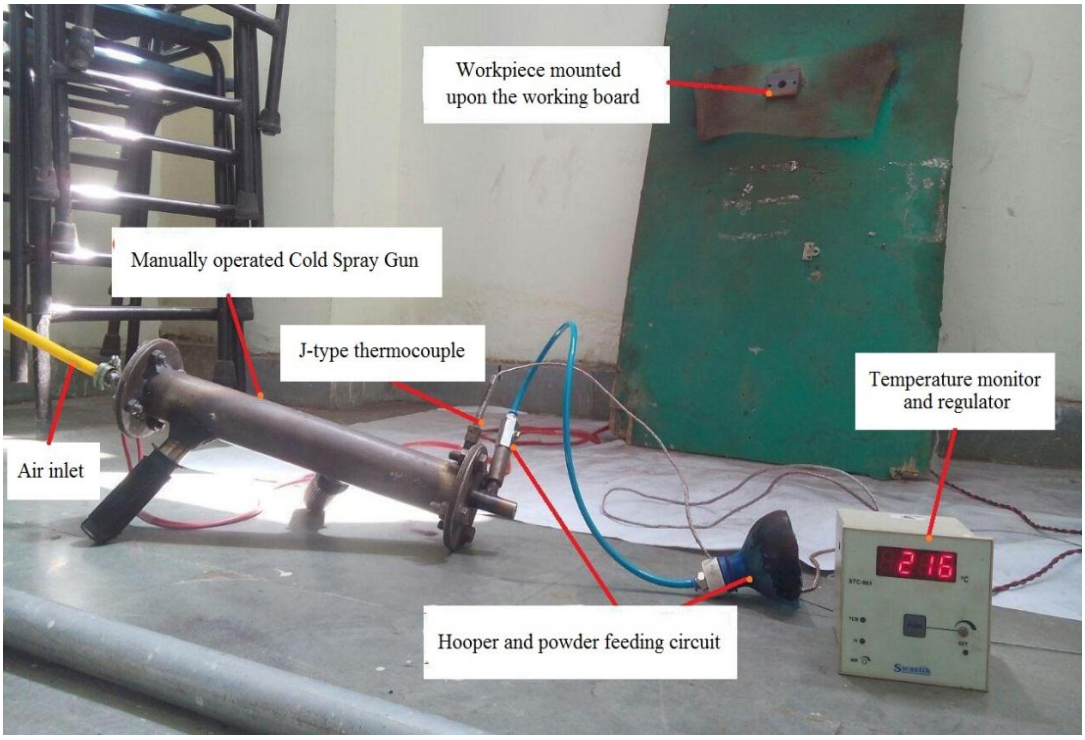

FIGURE 26 PHOTOGRAPH OF THE COMPLETE COLD SPRAY SYSTEM

DESIGN OF WORKPIECES

The technology being devised is focused upon reduction of time and capital that is incurred in making the molds manufacturing of day-to-day use items. After researching through the nearby industries, it was found that the plastic products were being manufactured by injection molding technique due to its versatility and accuracy. For a moderate product like fan speed regulator socket board, not much variety was found with the manufacturer because of the cost and intricacy of the molds. Since the molds were being manufactured with conventional material removal processes, the process time, material wastage and hence the cost was evaluated very high. In order to validate the hypothesis, such pattern was the need of experimentation. So, after having deep-in research of the problem of injection molding industry, a regular size 'fan speed regulator socket board' was selected. The CAD model has been shown in the figure 28. The same CAD model was converted into sliced thin layer format to feed into the fused deposition modelling machine. Figure 29 shows SolidWorks® stipulated mass properties of the workpiece.

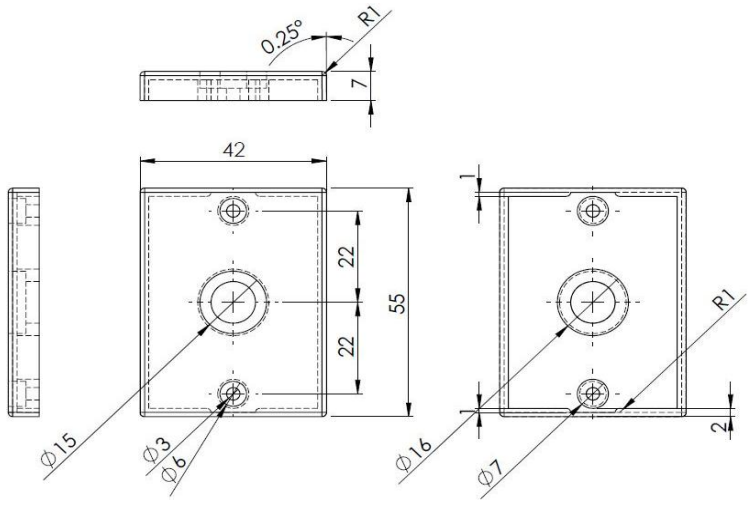

FIGURE 27 TWO-DIMENSIONAL DRAWING OF WORKPIECE PATTERN SHOWING ALL DIMENSIONS

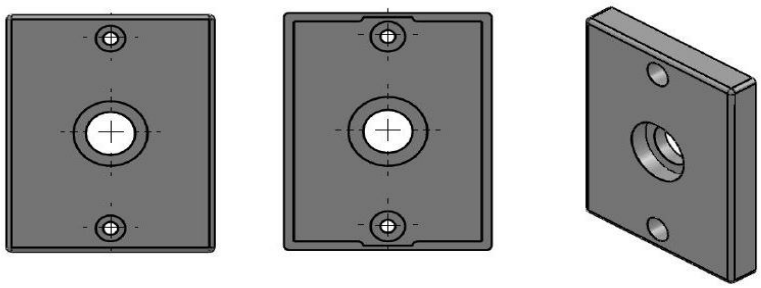

FIGURE 28 CAD MODEL OF THE WORK PIECE PATTERN

Mass properties of Part1 (Part Configuration - Default)

Output coordinate System: -- default --

Density = 0.00 grams per cubic millimeter

Mass = 6.49 grams

Volume = 6486.52 cubic millimeters

Surface area = 7552.58 millimeters^2

Center of mass: (millimeters)
X = 0.00
Y = 0.00
Z = 4.64

Principal axes of inertia and principal moments of inertia: (grams * square millimeters)
Taken at the center of mass.

Ix = (0.00, 1.00, 0.00)	Px = 1220.30
Iy = (-1.00, 0.00, 0.00)	Py = 1960.44
Iz = (0.00, 0.00, 1.00)	Pz = 3127.83

Moments of inertia: (grams * square millimeters)
Taken at the center of mass and aligned with the output coordinate system.

Lxx = 1960.44	Lxy = -0.00	Lxz = 0.00
Lyx = -0.00	Lyy = 1220.30	Lyz = 0.00
Lzx = 0.00	Lzy = 0.00	Lzz = 3127.83

Moments of inertia: (grams * square millimeters)
Taken at the output coordinate system.

Ixx = 2100.19	Ixy = -0.00	Ixz = 0.00
Iyx = -0.00	Iyy = 1360.05	Iyz = 0.00
Izx = 0.00	Izy = 0.00	Izz = 3127.83

FIGURE 29 SOLIDWORKS® STIPULATED MASS PROPERTIES OF THE WORKPIECE

PREPARATION OF WORKPIECES

The designed workpiece were printed in three dimensions using Fused Deposition Modelling machine. Figure 30 shows the photograph of ABS workpieces and figure 31 shows the fused deposition modelling of ABS workpieces. Few out of printed pieces were electroplated for surface enhancement. Figure 32 shows the electroplating apparatus in action and figure 33 shows the electroplated workpieces.

FIGURE 30 PHOTOGRAPHS OF RAW ABS WORKPIECES

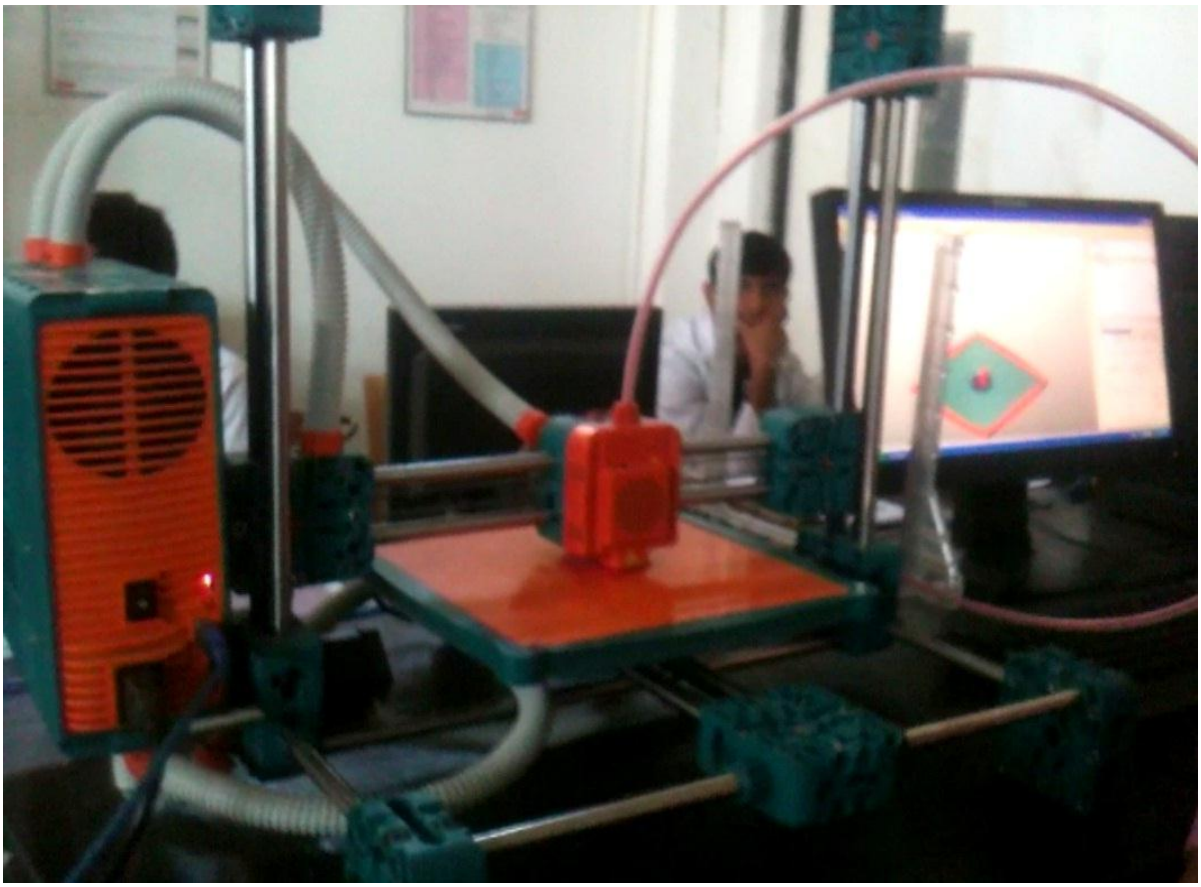

FIGURE 31 PHOTOGRAPH OF FUSED DEPOSITION MODELLING OF WORKPIECES

FIGURE 32 PHOTOGRAPH OF ELECTROPLATING APPARATUS

FIGURE 33 PHOTOGRAPHS OF ELECTRO-PLATED WORKPIECES

DESIGN OF EXPERIMENTS

While designing the experiments, persistent changes are made to the input variables of a process so that we may observe and identify corresponding effects on the output responses. In this study, 3 factors (Gas temperature, Electroplating thickness and Nozzle distance) each at 3 different levels are selected for experimentation to determine their effects upon surface roughness, deposition thickness and hardness.

TABLE 8 FACTORS AND LEVELS FINALIZED FOR THE EXPERIMENTATION

Parameter	Level 1	Level 2	Level 3
Gas Temperature, T (°C)	300	350	400
Electro-plating Thickness (microns)	100	300	600
Standoff Distance (mm)	15	20	25

For proper randomization and application of Taguchi technique, software MINITAB® was incorporated in the study to design the experiments. Figure 34 show the screenshot of the MINITAB® software interface meanwhile designing of experiments.

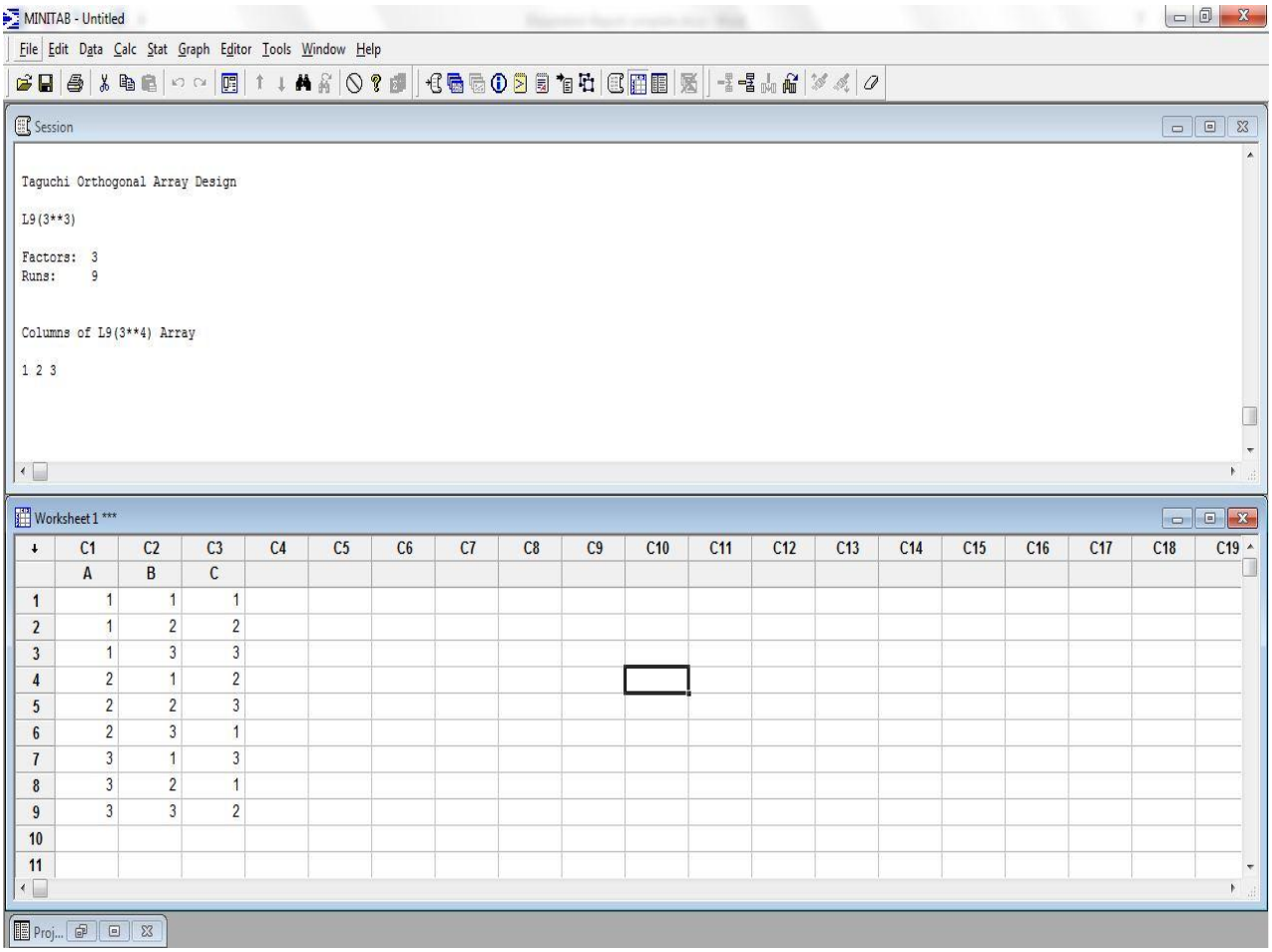

FIGURE 34 MINITAB® INTERFACE SHOWING DESIGN OF EXPERIMENTS

The experiments are framed according to Taguchi's L9 orthogonal array, as shown in table 11:-

TABLE 9 DESIGN OF EXPERIMENTS USING TAGUCHI'S L9 ORTHOGONAL ARRAY

Experiment No.	Gas Temperature	Electro-plating Thickness	Standoff Distance
1	300	100	15
2	300	300	20
3	300	600	25
4	350	100	20
5	350	300	25
6	350	600	15
7	400	100	25
8	400	300	15
9	400	600	20

EXPERIMENTATION

99.96% pure copper spherical powder with particle size of 400 mesh/37 micron was used to perform the trials. Total 36 trials were performed taking four samples for each experiment and the mean of each batch was taken to plot the results. Figure 35 shows the photograph of cold spray apparatus in action. Figure 36 shows the photograph of prepared workpieces. Figure 37 shows photographs of in process, workpiece.

FIGURE 35 PHOTOGRAPH OF COLD SPRAY APPARATUS IN ACTION

FIGURE 36 PHOTOGRAPHS SHOWING PREPARED SAMPLES USING COLD SPRAY

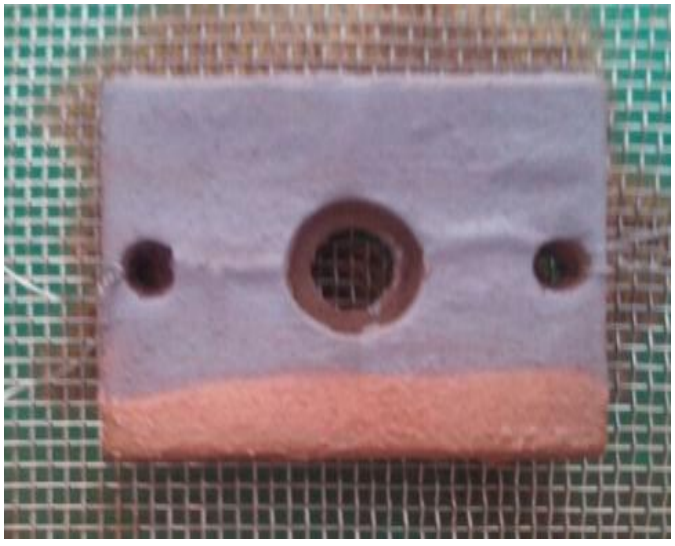

FIGURE 37 PHOTOGRAPHS OF IN PROCESSWORKPIECE

FIGURE 38 PHOTOGRAPHS OF POST PROCESS (A) BARE, (B) ELECTROPLATED (C) DAMAGED WORKPIECES

TESTING

After performing the trials, the final workpieces were subjected to surface roughness testing (figure 39), coating thickness testing (figure 40) and hardness testing (figure 41).

- Surface roughness test

FIGURE 39 PHOTOGRAPH SHOWING SURFACE ROUGHNESS TEST

- Thickness test

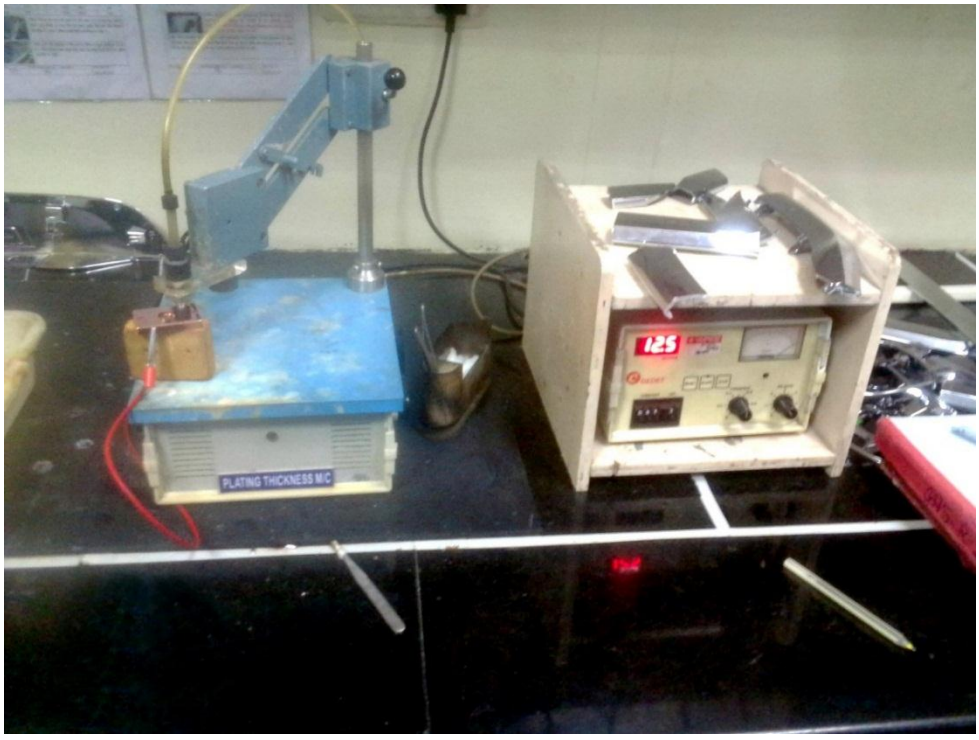

FIGURE 40 PHOTOGRAPH SHOWING COATING THICKNESS TEST

- Hardness test

FIGURE 41 PHOTOGRAPH SHOWING HARDNESS TEST

In this chapter, the effect of individual process parameters on the selected response characteristics has been discussed. The standard procedure suggested by Taguchi is employed. The mean or the average values and interaction plot of the response characteristics for each parameter at different levels have been calculated from experimental data. ANOVA of the experimental data has been done to calculate the contribution of each factor in each response and to check the significance of the model. The most favorable conditions (optimal settings) of the process parameters in terms of mean response of characteristic have been established by analyzing response curves.

The main effects indicate the general trends of influence of each parameter. The analysis of variance (ANOVA) is the statistical treatment most commonly applied to the results of the experiments in determining the percent contribution of each parameter against a stated level of confidence. Study of ANOVA table for a given analysis helps to determine which of the parameter need control. Results are divided into three sections on the basis of the three measured output responses.

1. Surface roughness
2. Thickness
3. Hardness

4.1 SURFACE ROUGHNESS:

In this section, the effect of process parameters that are gas temperature, electroplating thickness, and nozzle distance has been discussed and the experimental results are tabulated in table 10.

TABLE 10 RESULTS FOR SURFACE ROUGHNESS

Exp. No.	Gas Temp. (°C)	Electro-plating Thickness (microns)	Standoff Distance (mm)	Surface roughness (µm)
1	300	100	15	2.08
2	300	300	20	2.33
3	300	600	25	3.16
4	350	100	20	2.3
5	350	300	25	2.99
6	350	600	15	1.98
7	400	100	25	2.11
8	400	300	15	1.82
9	400	600	20	2.03

By using the MINITAB® software, the main effects and the interaction effects of the mean are evaluated and the results are represented graphically as follows:

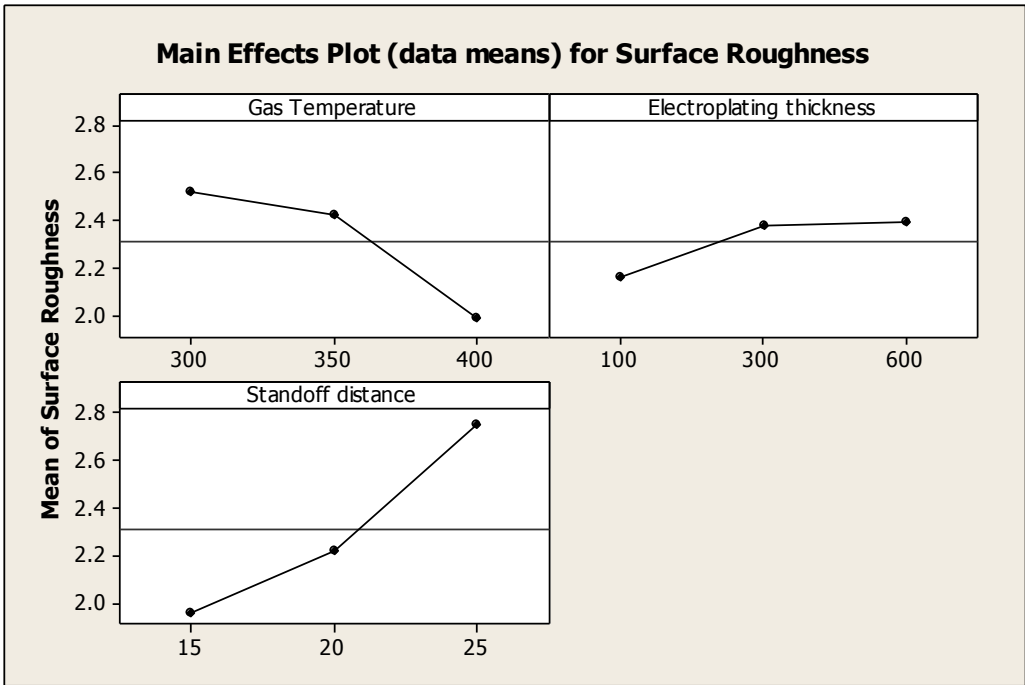

FIGURE 42 MAIN EFFECT PLOT FOR SURFACE ROUGHNESS

From the main effect plot it is interpreted that the surface roughness is decreasing as the temperature increases from 300°C to 400°C. This is expected as with increase in temperature, the impact energy of the bombarding particles also increases and hence the surface irregularities are less.

The minimum surface roughness is observed when the workpiece is electroplated with layer of up to 100 microns. With an increase in the electroplating thickness from 100 microns to 300 microns, the surface roughness also increases but there is no significant change when the thickness is further increased to 600 microns.

The stand-off distance plays a major role in determining surface roughness. As the standoff distance increases, the surface roughness also increases. This is possibly due to greater scattering of particles from larger stand-off distances. The least surface roughness values of 1.98 µm was achieved at the minimum standoff distance of 15mm.

From figure 43, one can interpret that all the three process parameters has direct impact on the surface roughness.

The optimized settings for surface roughness are 100micron electroplating thickness, 400°C gas temperature and 15mm standoff distance.

In order to effectively study the effect of each parameter with respect to other parameters the interaction effects has been plotted and is as follows:

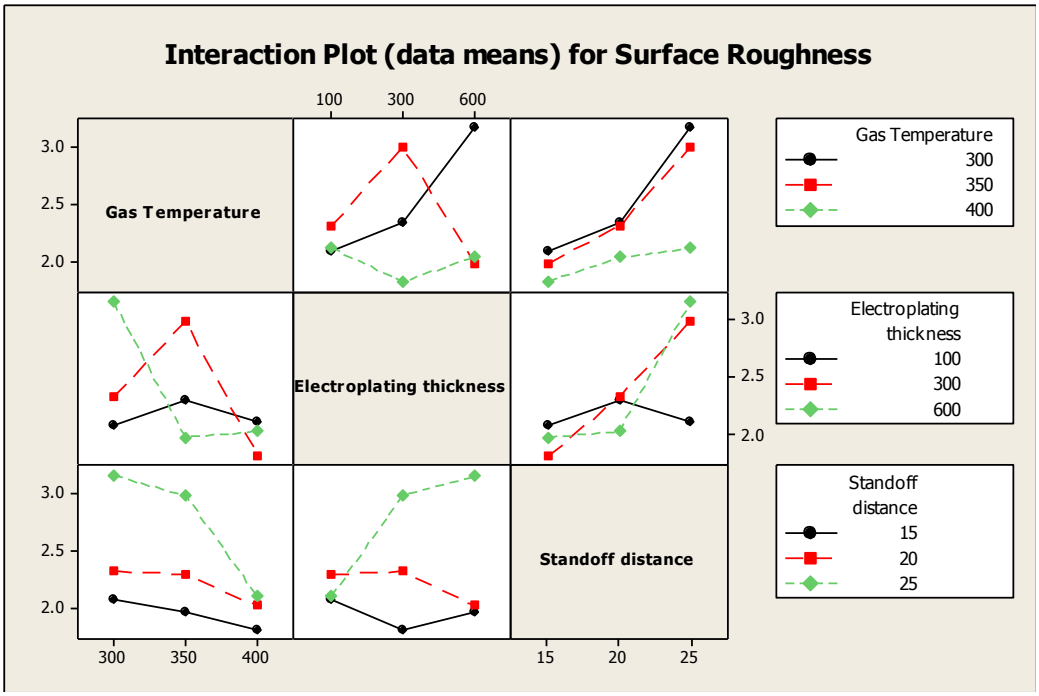

FIGURE 43 INTERACTION PLOT FOR SURFACE ROUGHNESS

From the interaction plot we can draw the optimized parameters for all the input variables with respect to other variables which give the more detailed information. From the interaction plot of means of surface roughness, it can be interpreted that there is a significant interaction between all the factors as there are very few parallel lines in the entire interaction plot. This implies that one factor is dependent upon another factor.

TABLE 11 ANALYSIS OF VARIANCE FOR SURFACE ROUGHNESS, USING ADJUSTED SS FOR TESTS

Source	DF	Seq SS	Adj SS	Adj MS	F	P	% contribution
Electroplating thickness	2	0.48869	0.48869	0.24434	3.56	0.219	28.65
Gas Temperature	2	0.09842	0.09842	0.04921	0.72	0.582	5.77
Standoff distance	2	0.98142	0.98142	0.49071	7.16	0.123	57.54
Error	2	0.13716	0.13716	0.06858			
Total	8	1.70569					
S = 0.261874 R-Sq = 91.96% R-Sq(adj) = 67.84%							
DF-degrees of freedom, SS-Sum of squares, MS-mean square (Variance) F-ratio of variance of a source to variance of error, P determines significance of a factor at 95% confidence level.							

The experiment data is analyzed by ANOVA at 95% confidence level and the contribution of each factor to the output response has been determined and the results are tabulated in table 11. The variation data for each factor and their interactions were F-tested to find significance of each. The principle of the F-test is that the larger the F values for a particular parameter, the greater is the effect on the performance characteristic due to the change in that process parameter. From table 11, it is clearly visible that surface roughness is mostly affected by electroplating thickness and standoff distance and gas temperature has least effect on it. We can see that standoff distance is the major contributing factor having percentage contribution of 57.54%, so it is important factor to be considered for surface roughness.

The parameter R^2 (amount of variation) =91.96%, Adj R^2 = 67.84%, and the standard deviation of error in the modelling, S= 0.261874.

The residual plot implies us about the variation with respect to each contributing factor. It should be minimum enough or should be close to mean line of graph, which implies that there is least variation in the experimental work. Figure 44 shows the residual plot for surface roughness.

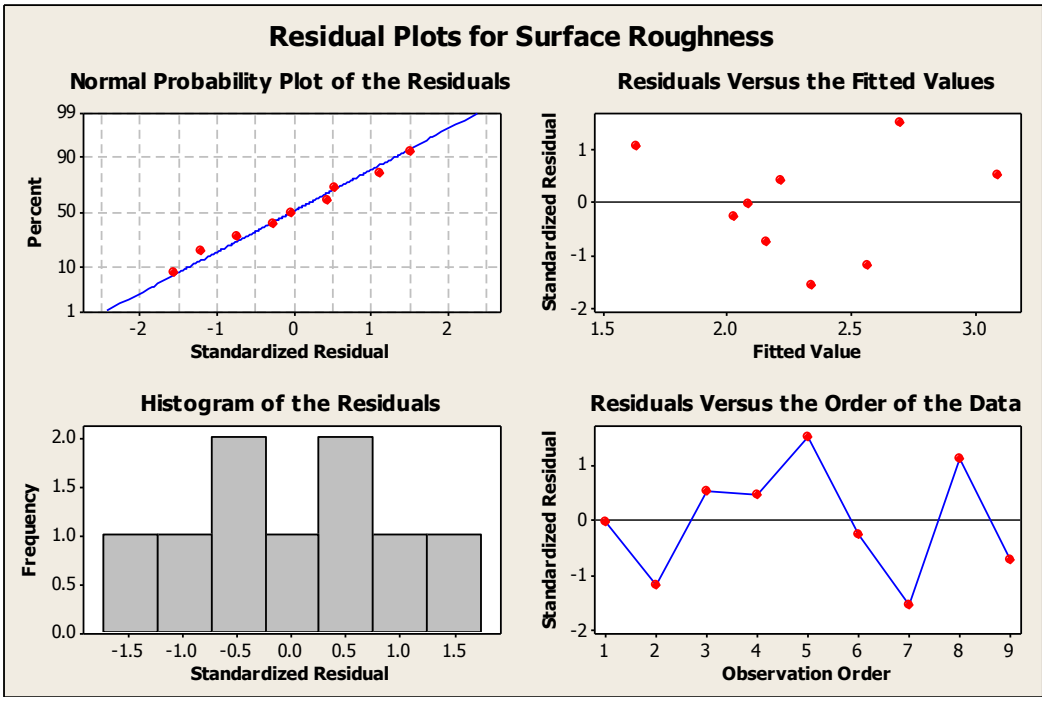

FIGURE 44 RESIDUAL PLOT FOR SURFACE ROUGHNESS

4.2 COATING THICKNESS

In this section, the effect of process parameters upon coating thickness is discussed. The results are tabulated in table 12.

TABLE 12 RESULTS FOR COATING THICKNESS

Exp. No.	Gas Temp. (°C)	Electro-plating Thickness (microns)	Standoff Distance (mm)	Coating thickness (mm)
1	300	100	15	0.86
2	300	300	20	1.08
3	300	600	25	0.65
4	350	100	20	1.23
5	350	300	25	0.71
6	350	600	15	0.91
7	400	100	25	0.78
8	400	300	15	0.99
9	400	600	20	1.62

From the main effect plot for thickness (figure 45), it is observed that with change in gas temperature, there is a noticeable change in coating thickness but with increase in electroplating thickness, there is no significant change in the coating thickness. Standoff distance plays a vital role in depositing the coating. As distance is increased from 15 mm to 20 mm standoff, the coating thickness increases and from 20mm to 25mm, it decreases.

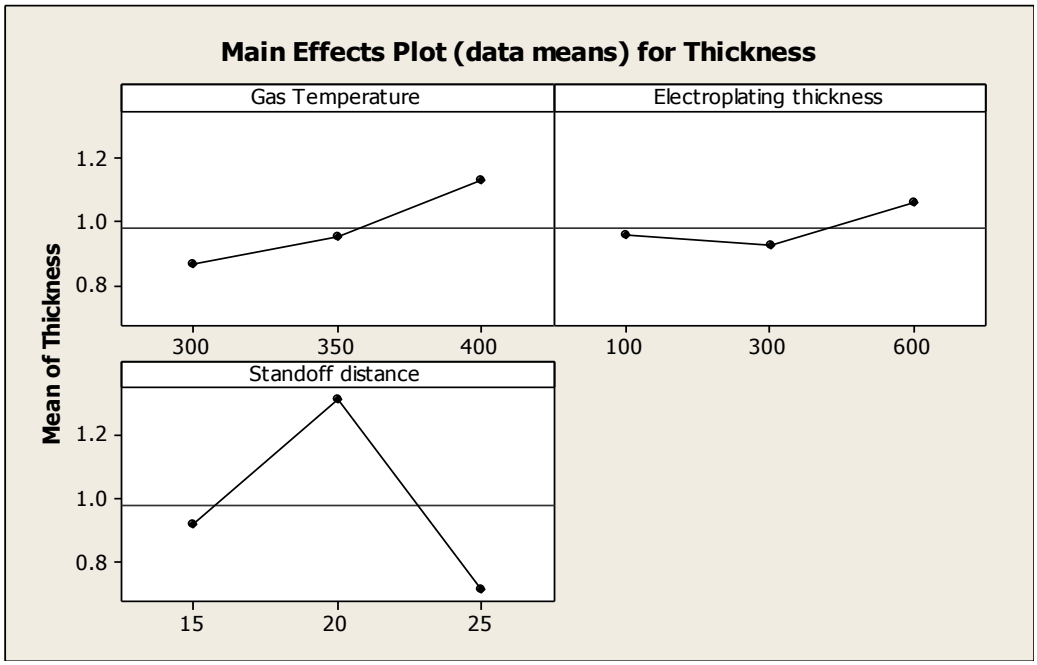

FIGURE 45 MAIN EFFECT PLOT FOR THICKNESS

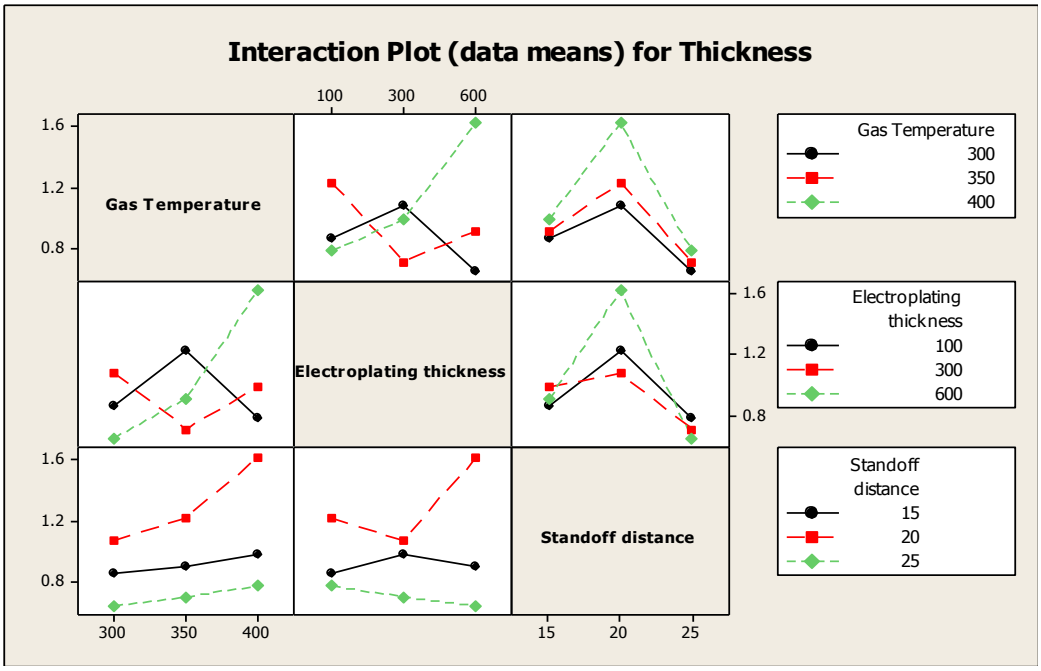

FIGURE 46 INTERACTION PLOT FOR THICKNESS

From the interaction plot we can draw the optimized parameters for all the input variables with respect to other variables which give the more detailed information. From the interaction plot of means of coating thickness, it can be interpreted that there is a significant interaction between all the factors as there are very few parallel lines in the entire interaction plot. This implies that one factor is dependent upon another factor.

TABLE 13 ANALYSIS OF VARIANCE FOR COATING THICKNESS, USING ADJUSTED SS FOR TESTS

Source	DF	Seq SS	Adj SS	Adj MS	F	P	% contribution
Electroplating thickness	2	0.11102	0.11102	0.05551	3.46	0.224	15.35
Gas Temperature	2	0.02936	0.02936	0.01468	0.91	0.522	4.06
Standoff distance	2	0.55082	0.55082	0.27541	17.17	0.055	76.15
Error	2	0.03209	0.03209	0.01604			
Total	8	0.72329					
S = 0.126667 R-Sq = 95.56% R-Sq(adj) = 82.25% DF-degrees of freedom, SS-Sum of squares, MS-mean square (Variance) F-ratio of variance of a source to variance of error, P determines significance of a factor at 95% confidence level.							

The experiment data is analyzed by ANOVA at 95% confidence level and the contribution of each factor to the output response has been determined and the results are tabulated in table 13. The

variation data for each factor and their interactions were F-tested to find significance of each. The principle of the F-test is that the larger the F values for a particular parameter, the greater is the effect on the performance characteristic due to the change in that process parameter. From table 13, it is clearly visible that coating thickness is mostly affected by standoff distance and gas temperature and electroplating thickness have least effect on it. We can see that standoff distance is the major contributing factor having percentage contribution of 76.15%, so it is important factor to be considered for coating thickness.

The parameter R^2 (amount of variation) =95.56%, Adj R^2 = 82.25%, and the standard deviation of error in the modelling, S= 0.126667.

The residual plot implies us about the variation with respect to each contributing factor. It should be minimum enough or should be close to mean line of graph, which implies that there is least variation in the experimental work. Figure 47 shows the residual plot for coating thickness.

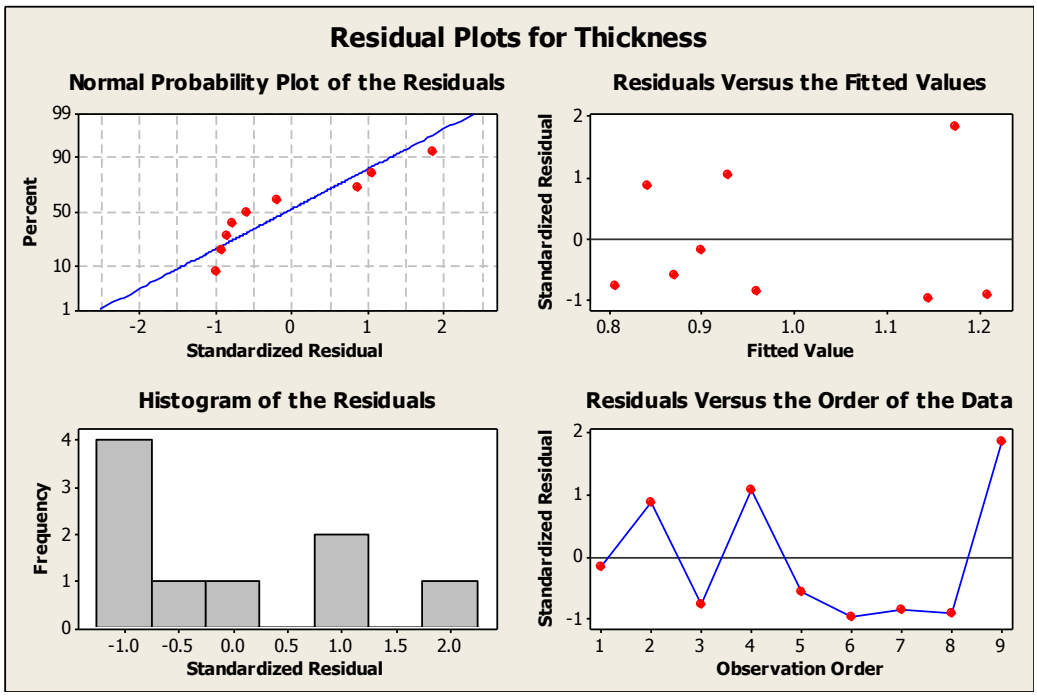

FIGURE 47 RESIDUAL PLOTS FOR COATING THICKNESS

4.3 HARDNESS

In this section, the effect of process parameters upon coating hardness is discussed. The results are tabulated in table 14.

TABLE 14 RESULTS FOR HARDNESS

Exp. No.	Gas Temp. (°C)	Electro-plating Thickness (microns)	Standoff Distance (mm)	Hardness (HRB)
1	300	100	15	57
2	300	300	20	32
3	300	600	25	22
4	350	100	20	37
5	350	300	25	28
6	350	600	15	62
7	400	100	25	33
8	400	300	15	66
9	400	600	20	48

From the main effect plot for hardness (figure 48), it is observed that the coating hardness is adversely affected with the change in gas temperature and the standoff distance, but the electroplating thickness affects it a very little.

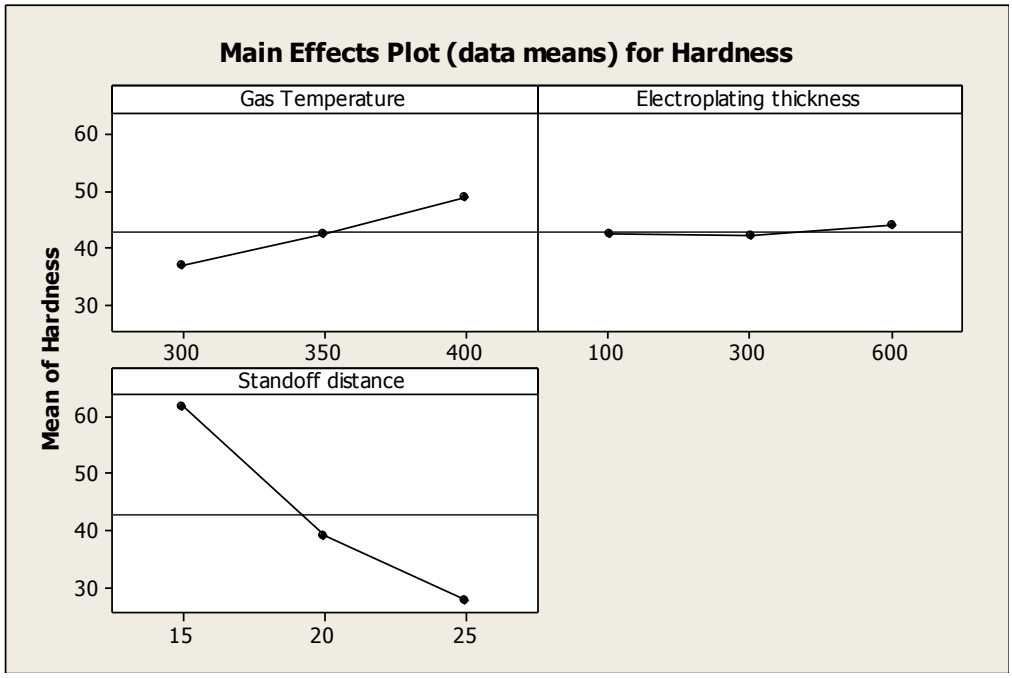

FIGURE 48 MAIN EFFECT PLOT FOR HARDNESS

FIGURE 49 INTERACTION PLOT FOR HARDNESS

From the interaction plot we can draw the optimized parameters for all the input variables with respect to other variables which give the more detailed information. From the interaction plot of means of coating thickness, it can be interpreted that there is a significant interaction between all the factors as there are very few parallel lines in the entire interaction plot. This implies that one factor is dependent upon another factor.

TABLE 15 ANALYSIS OF VARIANCE FOR HARDNESS, USING ADJUSTED SS FOR TESTS

Source	DF	Seq SS	Adj SS	Adj MS	F	P	% contribution
Electroplating thickness	2	216.89	216.89	108.44	18.77	0.051	10.66
Gas Temperature	2	6.89	6.89	3.44	0.60	0.627	0.33
Standoff distance	2	1798.22	1798.22	899.11	155.62	0.006	88.42
Error	2	11.56	11.56	5.78			
Total	8	2033.56					
S = 2.40370 R-Sq = 99.43% R-Sq(adj) = 97.73%							
DF-degrees of freedom, SS-Sum of squares, MS-mean square (Variance) F-ratio of variance of a source to variance of error, P determines significance of a factor at 95% confidence level.							

The experiment data is analyzed by ANOVA at 95% confidence level and the contribution of each factor to the output response has been determined and the results are tabulated in table 15. The variation data for each factor and their interactions were F-tested to find significance of each. The principle of the F-test is that the larger the F values for a particular parameter, the greater is the effect on the performance characteristic due to the change in that process parameter. From table 15, it is clearly visible that hardness is mostly affected by standoff distance and gas temperature and electroplating thickness have least effect on it. We can see that standoff distance is the major contributing factor having percentage contribution of 88.42%, so it is important factor to be considered for hardness.

The parameter R^2 (amount of variation) =99.43%, Adj R^2 = 97.73%, and the standard deviation of error in the modelling, S= 2.40370.

The residual plot implies us about the variation with respect to each contributing factor. It should be minimum enough or should be close to mean line of graph, which implies that there is least variation in the experimental work. Figure 47 shows the residual plot for coating thickness.

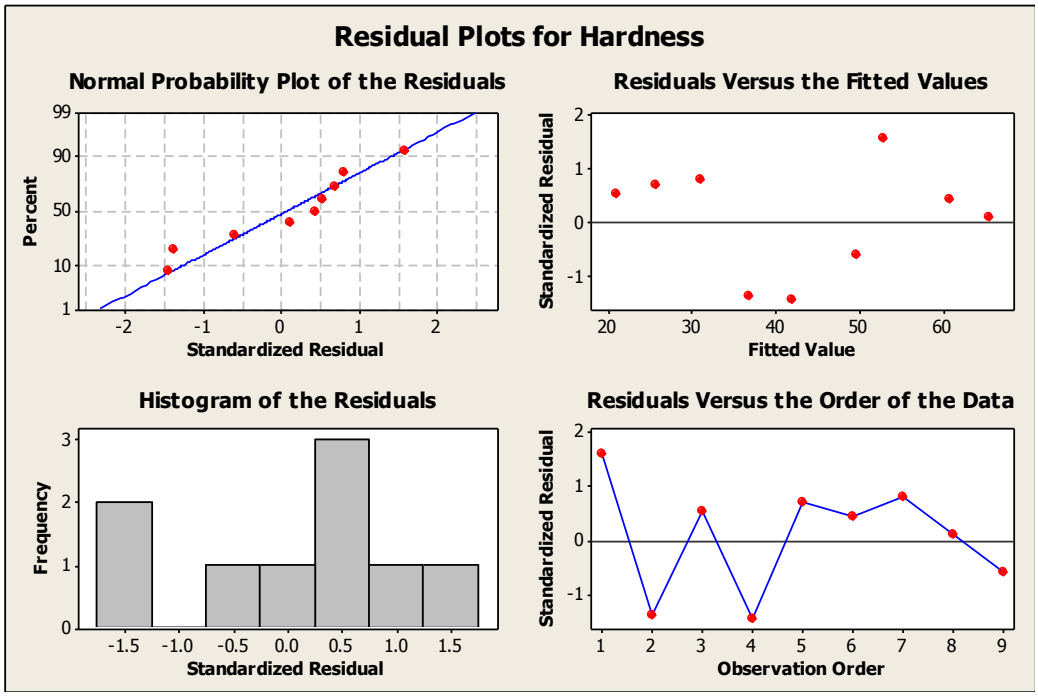

FIGURE 50 RESIDUAL PLOTS FOR HARDNESS

5.1 CONCLUSIONS

The trials of Gas Dynamics Cold Spray made upon the coated samples yielded successful results i.e. the thick coating was successfully formed and the penetration of the copper particles in the pattern bulk was estimated to be up to 3 microns of depth. So, it has been concluded that the bare patterns can withstand the high impact energy of the bombarding particles but they end up losing their surface properties. Whereas the specimen with an electro-plated layer up to 150 microns and above are suitably sound to be worked upon further to form molds. It is also evident from the trials that the surface properties of the plastic substrate are adversely affected by the number of scan passes of the gun. As visible in figure 38 (C), with increasing passes, the deterioration of the workpiece become evident.

From the trials, least surface roughness of 1.82 was achieved at 400 °C, on 300microns thick electroplated sample from the nozzle distance of 15mm. Whereas, the thickest coating of 1.62mm was achieved on 600 microns thick electroplated sample from the nozzle distance of 20mm with gas temperature of 400 °C. The hardness of 66Hrb was evident on the samples with 300 micron electroplating, sprayed with 400 °C from a distance of 15mm.

The optimized settings for surface roughness are 100micron electroplating thickness, 400°C gas temperature and 15mm standoff distance.

It can be inferred from the study that, the best optimum parameters to deposit thick layer of copper over ABS for mold formation are 600microns electroplating thickness, 400 °C gas temperature and 20mm standoff distance.

5.2 FUTURE SCOPES

The study could be further taken to the finding of optimized parameters like spray angle; materials for spray; pre-heating temperatures; number of scan passes, minimal pressure and velocity values for proper adhesion; particle size; and sintering temperature etc. Further, study could be extended to find better extraction and strengthening techniques for the molds. Moreover, the study is being carried over the patterns made by fused deposition modelling; there is huge scope in carrying similar study on the patterns made by other Rapid Prototyping Techniques.

REFERENCES

[1] Image courtesy:- http://www.ecvv.com

[2] Rapid Prototyping and Manufacturing-Reading material for IC training modules, Industrial Centre, The Hong Kong Polytechnic University

[3] Custom Part Net, 2008

[4] Chua et al,Rapid Prototyping: Principles and Applications in Manufacturing, World Scientific.

[5] D.T. Pham and R.S. Gault, International Journal of Machine Tools & Manufacture (1998)

[6] S. Au et al, A comparative study of rapid prototyping technology, Proceedings ASME Winter Conference,New Orleans, November 1993, vol. 66, pp. 73–82.

[7] Stratasys Inc., Fused deposition modelling for fast, safe plastic models, 12th Annual Conference on Computer Graphics, Chicago, April 1991, pp. 326–332.

[8] Chee Kai Chua et al(2003). Rapid Prototyping. World Scientific.

[9] https://thre3d.com/how-it-works/material-extrusion/fused-deposition-modeling-fdm

[10] Custom Part Net, 2008

[11] http://designinsite.dk/htmsider/m0007.htm

[12] William Callister. (7th Ed.). (2007). (Ch-14) Material science and engineering. Willey publication

[13] J. Karthikeyan, Advanced Materials and Processes (2006)

[14] V. K. Jr.Champagne et al, Journal of Thermal Spray Technology, 14(3) (2005) 330

[15] H. Singh et al, Frattura ed Integrità Strutturale, 22 (2012) 69-84; DOI: 10.3221/IGF-ESIS.22.08

[16] Sulzer Metco corporation

[17] H. Singh et al, Frattura ed Integrità Strutturale, 22 (2012) 69-84; DOI: 10.3221/IGF-ESIS.22.08

[18] V. K. Jr.Champagne et al, Journal of Thermal Spray Technology, 14(3) (2005) 330

[19] M. E.Dickinson et al, Nanoscience and Nanotechnology Letters, 2(4) (2010) 348.

[20] R. S. Lima et al, Thin Solid Films, 416 (2002) 129.

[21] V. K. Jr.Champagne et al, Journal of Thermal Spray Technology, 14(3) (2005) 330.

[22] V. K. Jr.Champagne et al, Journal of Thermal Spray Technology, 14(3) (2005) 330

[23] Sidhu T.S. PhD Thesis, 2006.

[24] Yoshio Tanaka, Epoxy Resins Chemistry and technology, Synthesis and Characterization of Epoxides pp 54 to 63

[25] William Callister. (7th Ed.). (2007). (Ch-14) Material science and engineering. Willey publication

[26] A. Rosochowski, et al Journal of Materials Processing Technology (2000)

[27] Pulak M. Pandey, Rapid prototyping technologies, applications and part deposition planning

[28] Chua, C.K., Leong, K.F. (2000) Rapid Prototyping: Principles and Applications in Manufacturing, World Scientific.

[29] D.T. Pham, R.S. Gault / International Journal of Machine Tools & Manufacture 38 (1998) 1257–1287

[30] S. Au, P.K. Wright, A comparative study of rapid prototyping technology, Proceedings ASME Winter Conference, New Orleans, November 1993, vol. 66, pp. 73–82.

[31] Chee Kai Chua; Kah Fai Leong, Chu Sing Lim (2003). Rapid Prototyping. World Scientific.

[32] J. Karthikeyan, Advanced Materials and Processes (2006)
[33] V. K. Jr.Champagne et al, Journal of Thermal Spray Technology, 14(3) (2005) 330.
[34] Knight, Thermal Spray: Past, Present and Future: A Look at Canons and Nanosplats
[35] Mitchell R. Dorfman, Global Turbine Sales Support, Sulzer Metco (US) Inc., Westbury, New York 405
[36] H. Singh et al, Frattura ed Integrità Strutturale, 22 (2012) 69-84; DOI: 10.3221/IGF-ESIS.22.08
[37] J. Pattison et al. / International Journal of Machine Tools & Manufacture 47 (2007) 627–634
[38] T. Stoltenhoff, H. Kreye, and H.J. Richter, An Analysis of the Cold Spray Process and Its Coatings
[39] S. Grigoriev et al. / Surface & Coatings Technology
[40] OH. Fukanuma, R.Z Huang, A Study on the Tensile Strength of Coatings Prepared by Cold Spray
[41] Shuo Yin, Yan Sun, Xiaofang Wang, Zhiwei Guo, and Hanlin Liao, Effect of Spray Angle on Temperature Distribution within the Metallic Substrate in Cold Spraying
[42] Hyun-Boo Jung et al, Effect of the Expansion Ratio and Length Ratio on a Gas-Particle Flow in a Converging-Diverging Cold Spray Nozzle
[43] K. Sakaki and Y. Shimizu, Effect of the Increase in the Entrance Convergent Section Length of the Gun Nozzle on the High-Velocity Oxygen Fuel and Cold Spray Process
[44] S. Yin et al. / Computational Materials Science 90 (2014) 7–15
[45] Hiroshi KATANODA et al. Experimental Study on Shock Wave Structures in Constant-area Passage of Cold Spray Nozzle
[46] C.-J. Li, H.-T. Wang, Q. Zhang, G.-J. Yang, W.-Y. Li, and H.L. Liao, Influence of Spray Materials and Their Surface Oxidation on the Critical Velocity in Cold Spraying
[47] A. Sova et al, Influence of powder injection point position on efficiency of powder preheating in cold spray: Numerical study
[48] Moridi et al, Number of Passes and Thickness Effect on Mechanical Characteristics of Cold Spray Coating
[49] Xian-Jin Ning et al, Numerical Study of In-flight Particle Parameters in Low-Pressure Cold Spray Process
[50] G. Huang et al. / Journal of Materials Processing Technology 214 (2014) 2497–2504
[51] Zhenhua Cai, Sihao Deng, Hanlin Liao, Chunnian Zeng, and Ghislain Montavon, The Effect of Spray Distance and Scanning Step on the Coating Thickness Uniformity in Cold Spray Process
[52] R. Huang and H. Fukanuma, Study of the Influence of Particle Velocity on Adhesive Strength of Cold Spray Deposits
[53] X. Suo et al. / Surface & Coatings Technology (2014)
[54] Wen-Ya Li and Chang-Jiu Li, Optimal Design of a Novel Cold Spray Gun Nozzle at a Limited Space
[55] W.Y.Li and C.J.Li, "Optimal design of a novel cold spray gun nozzle at a limited space" Journal of Thermal spray technology, (14) (3) (2005) pp391-396
[56] H. Singh et al, Frattura ed Integrità Strutturale, 22 (2012) 69-84; DOI: 10.3221/IGF-ESIS.22.08

[57] Hezhou Ye , Jianfeng Wang, 'Preparation of aluminum coating on Lexan by cold spray', page no. (21-24)(2014).
[58] Maurice J.A.A. Goris, Ian J. Bennett and Wilma Eerenstein, ' Aluminum foil and cold spray copper technology as cost reduction process step in back-contact module design', page no. (342-347)(2014).
[59] Narinder Kaur, Manoj Kumar, Sanjeev K. Sharma, Deuk Young Kim, S. Kumar, N.M. Chavan, S.V. Joshi, Narinder Singh, Harpreet Singh, 'Study of mechanical properties and high temperature oxidation behavior of a novel cold-spray Ni-20Cr coating on boiler steels', page no. (13-25)(2014).
[60] A Sova, S. Grigoriev, A. Kochetkova, I. Smurov, 'Influence of powder injection point position on efficiency of powder preheating in cold spray: Numerical study', page no. (226-231)(2013).
[61] Michael Saleh, Vladimir Luzin, Kevin Spencer, 'Analysis of the residual stress and bonding mechanism in the cold spray technique using experimental and numerical methods', page no. (15-28)(2014).
[62] T. Hussain, D.G. McCartney, P.H. Shipway, D. Zhang, 'Bonding mechanisms in cold spraying: the contributions of metallurgical and mechanical components', page no. (364-378)(2008).
[63] V. Lemiale, P.C. King, M. Rudmana, M. Prakash, P.W. Cleary, M.Z. Jahedi, S. Gulizia, 'Temperature and strain rate effects in cold spray investigated by smoothed particle hydrodynamics', page no. (121-130)(2014).
[64] Renzhong Huang, Wenhua Ma, Hirotaka Fukanuma, 'Development of ultra-strong adhesive strength coatings using cold spray', page no. (832-841)(2014).
[65] J. Cizek, O.Man, P. Roupcova, K. Loke, I. Dlouhy, 'Oxidation performance of cold spray Ti–Al barrier coated γ-TiAl intermetallic substrates', page no. (1-5)(2014).
[66] J. Henao, A. Concustell, I.G. Cano, N. Cinca, S. Dosta, J.M. Guilemany, 'Influence of Cold Gas Spray process conditions on the microstructure of Fe-based amorphous coatings', page no.(995-999)(2014).
[67] M. Gardon, A. Concustell, S. Dosta, N. Cinca, I.G. Cano, J.M. Guilemany, 'Improved bonding strength of bioactive cermet Cold Gas Spray coatings', page no. (117-121)(2014).
[68] Edward Joshua T. Pialago, Chan Woo Park, 'Cold spray deposition characteristics of mechanically alloyed Cu-CNT composite powders', page no. (63-74)(2014).
[69] Sukhminderbir Singh Kalsi, T.S. Sidhu, H. Singh, J. Karthikeyan, 'Analysis of material degradation for uncoated and NiCoCrAlY cold spray coated Superfer 800H in the secondary chamber of medical waste incinerator', page no. (238-246)(2014).
[70] Gobinda C. Saha, A. Mateen, Tahir I. Khan, 'Tribological performance study of hvof-sprayed microstructured and nanostructured wc-17wt.% Co coatings', page no. (1-10)(2010).
[71] A Moridi, S. M. Hassani Gangaraj, S. Vezzu, M. Guagliano, 'Number of passes and thickness effect on mechanical', page no. (449-459)(2014).
[72] N. S. Cheruvu, K. S. Chan, D. W. Gandy, 'Effect of time and temperature on thermal barrier coating failure mode under oxidizing environment', page no. (1-7)(2014).
[73] Kanani, Nasser. 2005. Electroplating: Basic Principles, Processes and Practice. Oxford, U.K.: Elsevier Advanced Technology. ISBN 1856174514

[74] Poyner, J. 1986. Electroplating (Workshop Practice Series No. 11). TransAtlantic Publications. ISBN 0852428626

Hardness Conversion Chart for Copper

HV	HK	HRB	HRF	HR15T	HR30T	HR45T	HBS
126	133	66.6	97.9	87.1	68.7	48.0	118
124	131	65.2	97.2	86.7	67.7	46.7	116
122	129	63.8	96.4	86.4	66.8	45.3	113
120	127	62.3	95.7	86.0	65.8	43.8	111
118	125	60.7	94.9	85.6	64.8	42.4	109
116	122	59.0	94.0	85.2	63.7	40.9	106
114	120	57.3	93.1	84.8	62.6	39.3	104
112	118	55.4	92.2	84.3	61.4	37.7	102
110	116	53.5	91.2	83.8	60.2	36.0	100
108	114	51.5	90.2	83.3	58.9	34.3	97
106	111	49.4	89.1	82.8	57.6	32.5	95
104	109	47.2	87.9	82.2	56.3	30.6	93
102	107	44.9	86.7	81.5	54.8	28.7	91
100	104	42.5	85.5	80.8	53.4	26.7	88
98	102	39.9	84.1	80.2	51.8	24.6	86
94	100	37.3	82.7	79.4	50.2	22.4	84
96	98	34.5	81.2	78.6	48.5	20.0	82
92	95	31.7	79.7	77.7	46.8	17.6	80
90	93	28.7	78.0	76.7	44.9	15.1	77
88	91	25.6	76.3	75.7	43.0	12.4	75
86	88	22.5	74.5	74.6	41.1		73
84	86	19.2	72.6	73.4	39.0		71
82	83	15.8	70.6	72.1	36.8		69
80	81	12.4	68.5	70.6	34.6		67
78	79	8.8	66.3	69.1	32.3		64
76	76		64.1	67.5	29.8		62
74	74		61.8	65.7	27.3		60
72	71		59.3	63.8	24.7		58
70	69		56.8	61.8	21.9		56
68	66		54.3	59.7	19.0		54
66	64		51.6	57.5	16.0		52
64	61		48.8	55.2	12.9		50
62	59		46.0	52.9	8.2		47
60	56		43.1	50.5			45
58	53		40.1	48.1			43
56	51		36.9	45.6			41
54	48		33.7	43.1			
52	45		30.3	40.6			

Common Applications and Nomenclature for Hardness Tests

Test	Symbol	Indenter	Test Force (kg)	Indentation depth (mm)*	Application
Rockwell A	HRA	diamond	60	(100 - HRA value) / 500	Very hard materials, cemented carbides
Rockwell B	HRB	1/16" ball	100	(130 - HRB value) / 500	Low strength steel, copper alloys, aluminum alloys, malleable iron
Rockwell C	HRC	diamond	150	(100 - HRC value) / 500	High strength steel, titanium, pearlitic malleable iron
Rockwell D	HRD	diamond	100	(100 - HRD value) / 500	High strength steel, thin steel
Rockwell E	HRE	1/8" ball	100	(130 - HRE value) / 500	Cast iron, aluminum and magnesium alloys
Rockwell F	HRF	1/16" ball	60	(130 - HRF value) / 500	Annealed copper alloys, thin soft metals
Rockwell G	HRG	1/16" ball	150	(130 - HRG value) / 500	Phosphor bronze, beryllium copper, malleable irons**
Rockwell H	HRH	1/8" ball	60	(130 - HRH value) / 500	Aluminum, zinc, lead
Rockwell K	HRK	1/8" ball	150	(130 - HRK value) / 500	Bearing metals and other very soft or thin materials, including plastics. Use smallest ball and heaviest load that do not give anvil effect.
Rockwell L	HRL	1/4" ball	60	(130 - HRL value) / 500	
Rockwell M	HRM	1/4" ball	100	(130 - HRM value) / 500	
Rockwell P	HRP	1/4" ball	150	(130 - HRP value) / 500	
Rockwell R	HRR	1/2" ball	60	(130 - HRR value) / 500	
Rockwell S	HRS	1/2" ball	100	(130 - HRS value) / 500	
Rockwell V	HRV	1/2" ball	150	(130 - HRV value) / 500	
Superficial Rockwell N	HR15N	diamond	15	(100 - HR15N value) / 1000	Cemented carbides, thin steel and case hardened steel, hard cast irons, titanium, and other materials harder than 100HRB
Superficial Rockwell N	HR30N	diamond	30	(100 - HR30N value) / 1000	
Superficial Rockwell N	HR45N	diamond	45	(100 - HR45N value) / 1000	
Superficial Rockwell T	HR15T	1/16" ball	15	(100 - HR15T value) / 1000	Copper alloys, phosphor bronze, soft steels, aluminum alloys, malleable iron, thin soft sheet metals
Superficial Rockwell T	HR30T	1/16" ball	30	(100 - HR30T value) / 1000	
Superficial Rockwell T	HR45T	1/16" ball	45	(100 - HR45T value) / 1000	

Test	Symbol	Indenter	Test Force (kg)	Indentation depth (mm)*	Application
Superficial Rockwell W	HR15W	⅛" ball	15	(100 - HR15W value) / 1000	Cast iron, aluminum and magnesium alloys, bearing metals, zinc, lead
Superficial Rockwell W	HR30W	⅛" ball	30	(100 - HR30W value) / 1000	
Superficial Rockwell W	HR45W	⅛" ball	45	(100 - HR45W value) / 1000	
Superficial Rockwell X	HR15X	¼" ball	15	(100 - HR15X value) / 1000	
Superficial Rockwell X	HR30X	¼" ball	30	(100 - HR30X value) / 1000	
Superficial Rockwell X	HR45X	¼" ball	45	(100 - HR45X value) / 1000	
Superficial Rockwell Y	HR15Y	½" ball	15	(100 - HR15Y value) / 1000	
Superficial Rockwell Y	HR30Y	½" ball	30	(100 - HR30Y value) / 1000	
Superficial Rockwell Y	HR45Y	½" ball	45	(100 - HR45Y value) / 1000	
Vickers - "Macro"	HV	diamond	1-100	diagonal length in mm / 7	A wide range of materials
Vickers - "Micro"	HV	diamond	.005 to 1	diagonal length in mm / 7	A wide range of materials
Knoop	HK	diamond	.005 to 1	diagonal length in mm/ 30	A wide range of materials, case depth determination

Scale	Symbol	Indenter and Load force
Vickers	HV	Vickers diamond, nickel alloys (1, 5, 10 or 30-kgf), copper (100-gf), aluminum (15-kgf)
Knoop	HK	Knoop diamond, 500-gf and over
Rockwell A	HRA	Diamond, 60-kgf
Rockwell B	HRB	Steel ball 1/16", 100-kgf
Rockwell C	HRC	Diamond, 150-kgf
Rockwell D	HRD	Diamond, 100-kgf
Rockwell E	HRE	Steel ball ⅛", 100-kgf
Rockwell F	HRF	Steel ball 1/16", 60-kgf
Rockwell G	HRG	Steel ball 1/16", 150-kgf
Rockwell H	HRH	Steel ball ⅛", 60-kgf
Rockwell K	HRK	Steel ball ⅛", 150-kgf
Superficial Rockwell 15N	HR15N	Diamond, 15-kgf
Superficial Rockwell 30N	HR30N	Diamond, 30-kgf
Superficial Rockwell 45N	HR45N	Diamond, 45-kgf
Superficial Rockwell 15T	HR15T	Steel ball 1/16", 15-kgf
Superficial Rockwell 30T	HR30T	Steel ball 1/16", 30-kgf
Superficial Rockwell 45T	HR45T	Steel ball 1/16", 45-kgf
Superficial Rockwell 15W	HR15W	Steel ball ⅛", 15-kgf
Brinell	HBW	Tungsten carbide 10mm ball, 3000-kgf
Brinell	HBS	Steel 10mm ball, steel and nickel (3000-kgf), brass and aluminum (500-kgf)